



PNNL-32666

R-Value Measurements Performed on Uranium Targets Irradiated with Fission Spectrum Neutrons in FY 2021 for F2019 Project

March 2022

NE Uhnak
MM Haney
LR Greenwood
BD Pierson
JI Friese
LA Metz



Prepared for the U.S. Department of Energy
under Contract DE-AC05-76RL01830

DISCLAIMER

This report was prepared as an account of work sponsored by an agency of the United States Government. Neither the United States Government nor any agency thereof, nor Battelle Memorial Institute, nor any of their employees, makes **any warranty, express or implied, or assumes any legal liability or responsibility for the accuracy, completeness, or usefulness of any information, apparatus, product, or process disclosed, or represents that its use would not infringe privately owned rights.** Reference herein to any specific commercial product, process, or service by trade name, trademark, manufacturer, or otherwise does not necessarily constitute or imply its endorsement, recommendation, or favoring by the United States Government or any agency thereof, or Battelle Memorial Institute. The views and opinions of authors expressed herein do not necessarily state or reflect those of the United States Government or any agency thereof.

PACIFIC NORTHWEST NATIONAL LABORATORY
operated by
BATTELLE
for the
UNITED STATES DEPARTMENT OF ENERGY
under Contract DE-AC05-76RL01830

Printed in the United States of America

Available to DOE and DOE contractors from the
Office of Scientific and Technical Information,
P.O. Box 62, Oak Ridge, TN 37831-0062;
ph: (865) 576-8401
fax: (865) 576-5728
email: reports@adonis.osti.gov

Available to the public from the National Technical Information Service
5301 Shawnee Rd., Alexandria, VA 22312
ph: (800) 553-NTIS (6847)
email: orders@ntis.gov <<https://www.ntis.gov/about>>
Online ordering: <http://www.ntis.gov>

R-Value Measurements Performed on Uranium Targets Irradiated with Fission Spectrum Neutrons in FY 2021 for F2019 Project

March 2022

NE Uhnak
MM Haney
LR Greenwood
BD Pierson
JI Friese
LA Metz

Prepared for
the U.S. Department of Energy
under Contract DE-AC05-76RL01830

Pacific Northwest National Laboratory
Richland, Washington 99354

Summary

The separation and characterization of two irradiated uranium targets, a depleted uranium (DU) and a highly enriched uranium (HEU) target, was conducted in April of 2021. The two targets were assembled at Los Alamos National Laboratory (LANL) and irradiated using the critical assembly at the National Criticality Experiments Research Center (NCERC). Splits of the dissolved targets were received by Pacific Northwest National Laboratory (PNNL), after which the PNNL and LANL teams chemically separated the solutions using independent separation schemes and analyzed the separated fractions for short-lived actinides and fission products.

Chemical separations at PNNL were traced with stable or radioactive tracers to allow for the determination of chemical yields, analyzing using either inductively coupled plasma optical emission spectroscopy (ICP-OES), inductively coupled plasma mass spectrometry (ICP-MS) or gamma emission analysis (GEA), depending on the nature of the tracer. Several other analytical techniques were used by PNNL including kinetic phosphorescence analysis (KPA) and thermal ionization mass spectrometry (TIMS), depending on the analyte's need.

The teams compared current and historical PNNL and LANL data with literature values. Overall, there was agreement between the two laboratories for the bulk of analytes, with some notable exceptions such as ^{111}Ag , and $^{141,143,144}\text{Ce}$. These comparisons and analysis provided total atoms as well as the R-values for the short-lived actinides ^{237}U and ^{239}Np , and the fission products ^{89}Sr , ^{91}Y , $^{95/97}\text{Zr}$, ^{99}Mo , ^{111}Ag , $^{115/115\text{m}}\text{Cd}$, $^{136/137}\text{Cs}$, ^{140}Ba , $^{141/143/144}\text{Ce}$, ^{147}Nd , ^{153}Sm , ^{156}Eu , and ^{161}Tb . The data presented in this report represents the sixth NCERC irradiation of HEU and DU (FY 2013, FY 2014, FY 2015, FY 2017, FY 2018, FY 2021), and their subsequent separation and analysis.

Acknowledgments

A number of PNNL staff not listed as authors contributed to this work. The authors recognize the following list of staff members for chemically processing and analyzing the delivered samples using a multitude of analytical techniques as well as their diligence and attention to detail—all these skills were required to successfully complete this experiment.

The authors thank Ean Arnold, Chelsie Beck, James Bowen, Ronald Del Mar, Staci Herman, Lindsay Irwin, Bethany Lawler, Dawn Lucas, Matthew Risen-Huber, and Truc Trang-Le, and the radiochemistry team that contributed to this work in the past.

Acronyms and Abbreviations

CFY	cumulative fission yield
DU	depleted uranium
ENDF	Evaluated Nuclear Data File
FY	fiscal year
GEA	gamma energy analysis
HEDTA	hydroxyethylethylenediaminetriacetic acid
HEU	highly enriched uranium
ICP-MS	inductively coupled plasma mass spectrometry
ICP-OES	inductively coupled plasma optical emission spectroscopy
KPA	kinetic phosphoresce analysis
LANL	Los Alamos National Laboratory
LEGe	low energy germanium detector
LEPS	low energy photon spectroscopy
LSC	liquid scintillation counting
NCERC	National Criticality Experiments Research Center
PNNL	Pacific Northwest National Laboratory
RSD	relative standard deviation
TIMS	thermal ionization mass spectrometry

Contents

Summary.....	ii
Acknowledgments.....	iii
Acronyms and Abbreviations	iv
1.0 Introduction	1
2.0 Irradiation of Prepared Targets	2
2.1 Preparation of A Solution and Splits.....	2
3.0 Radiochemical Methodology.....	3
3.1 Radiochemical Processing at PNNL	3
3.1.1 Sample Splitting and Spiking	3
3.1.2 Analysis of A Solution	4
3.2 Radiochemical Separations	5
3.2.1 Separation Chemistry Methodology and Discussion	5
3.2.2 Analysis of Separated Fractions	7
4.0 R-value Calculation	9
5.0 Summary of FY 2021 Results	11
6.0 Comparison of FY 2021 Results to Historical Campaigns and Literature Values	17
6.1 Strontium-89.....	17
6.2 Yttrium-91	18
6.3 Zirconium-95	20
6.4 Zirconium-97	21
6.5 Ruthenium-103.....	22
6.6 Silver-111	23
6.7 Cadmium-115.....	24
6.8 Cadmium-115m.....	25
6.9 Tellurium-132	26
6.10 Cesium-136.....	27
6.11 Cesium-137	29
6.12 Barium-140.....	30
6.13 Cerium-141	31
6.14 Cerium-143	32
6.15 Cerium-144	33
6.16 Neodymium-147	34
6.17 Samarium-153.....	35
6.18 Europium-156.....	36
6.19 Terbium-161.....	37
6.20 Uranium-237	38
6.21 Neptunium-239.....	39

7.0	Result Highlights.....	40
8.0	Lessons Learned	41
9.0	Literature R-values.....	42
10.0	Specific Recommendations	44
11.0	Conclusions.....	45
12.0	References.....	46
	Appendix A – PNNL Calculations and Associated Uncertainty	A.1

Figures

Figure 3.1.	Radiochemical processing scheme at PNNL for dissolved A solutions of irradiated U target in FY 2021, process used for both DU and HEU targets.....	5
Figure 3.2.	Relative percent yield of each lanthanide fraction collected found in the HEU target.	7
Figure 6.1.	Strontium-89 R-values for DU and HEU samples irradiated on the Flattop critical assembly compared to previous R-value campaigns and ENDF (R $\pm 1\sigma$).	17
Figure 6.2.	Yttrium-91 R-values for DU sample irradiated on the Flattop critical assembly compared to previous R-value campaigns and ENDF (R $\pm 1\sigma$).	19
Figure 6.3.	Zirconium-95 R-values for DU and HEU samples irradiated on the Flattop critical assembly compared to previous R-value campaigns and ENDF (R $\pm 1\sigma$).	21
Figure 6.4.	Zirconium-97 R-values for DU and HEU samples irradiated on the Flattop critical assembly compared to previous R-value campaigns and ENDF (R $\pm 1\sigma$).	22
Figure 6.5.	Ruthenium-103 R-values for DU and HEU samples irradiated on the Flattop critical assembly compared to previous R-value campaigns and ENDF (R $\pm 1\sigma$).	23
Figure 6.6.	Silver-111 R-values for HEU and DU samples irradiated on Flattop critical assembly compared to previous R-value campaigns and ENDF (R $\pm 1\sigma$).	24
Figure 6.7.	Cadmium-115 R-values for DU and HEU samples irradiated on the Flattop critical assembly compared to previous R-value campaigns and ENDF V.III.0 (R $\pm 1\sigma$).	25
Figure 6.8.	Cadmium-115m R-values for DU and HEU samples irradiated on the Flattop critical assembly compared to previous R-value campaigns and JEFF-3.1.1 (R $\pm 1\sigma$).	26
Figure 6.9.	Tellurium-132 R-values for DU and HEU samples irradiated on the Flattop critical assembly compared to previous R-value campaigns and ENDF (R $\pm 1\sigma$).	27
Figure 6.10.	Left plot shows the Cs-136 R-values for DU sample, the right plot shows the HEU R-Values.	28

Figure 6.11. Cesium-137 R-values for DU and HEU samples irradiated on the Flattop critical assembly compared to previous R-value campaigns and ENDF (R $\pm 1\sigma$)	29
Figure 6.12. Barium-140 R-values for DU and HEU samples irradiated on the Flattop critical assembly compared to previous R-value campaigns and ENDF (R $\pm 1\sigma$)	30
Figure 6.13. Cerium-141 R-values for DU and HEU samples irradiated on the Flattop critical assembly compared to previous R-value campaigns and ENDF (R $\pm 1\sigma$)	31
Figure 6.14. Cerium-143 R-values for DU and HEU samples irradiated on the Flattop critical assembly compared to previous R-value campaigns and ENDF (R $\pm 1\sigma$)	32
Figure 6.15. Cerium-144 R-values for DU and HEU samples irradiated on the Flattop critical assembly compared to previous R-value campaigns and ENDF (R $\pm 1\sigma$)	33
Figure 6.16. Neodymium-147 R-values for DU and HEU samples irradiated on the Flattop critical assembly compared to previous R-value campaigns and ENDF (R $\pm 1\sigma$)	34
Figure 6.17. Samarium-153 R-values for DU sample irradiated on the Flattop critical assembly compared to previous R-value campaigns and ENDF (R $\pm 1\sigma$); open symbols denote R-Values calculated using the ^{153}Sm CFY reported in Jackson et al. 2018.	35
Figure 6.18. Europium-156 R-values for DU sample irradiated on the Flattop critical assembly compared to previous R-value campaigns and ENDF (R $\pm 1\sigma$)	36
Figure 6.19. Terbium-161 R-values for DU and HEU samples irradiated on the Flattop compared to previous R-value campaigns and ENDF (R $\pm 1\sigma$).	38

Tables

Table 2.1. Details on target including naming, mass, material, irradiation conditions, and dates.	2
Table 2.2. Isotopic composition in percent of the target materials.	2
Table 2.3. A solution splits sent to PNNL.	2
Table 3.1. PNNL A solution splits.	3
Table 3.2. Tracer spiking for Z11051 and Z11050 for the tracers ^{237}Np , $^{110\text{m}}\text{Ag}$, ^{109}Cd , ^{134}Cs , ^{152}Eu and stable tracers Sm, Eu, Tb, Y, and Sr.	3
Table 3.3. Dates for each GEA of A solutions for samples Z11050 and Z11051.	4
Table 3.4. PNNL A solution GEA used to quantify applicable radionuclides.	4
Table 3.5. Elution conditions for the separation of rare earth fission products on vacuum box.	6
Table 4.1. PNNL historical r-values.	9
Table 5.1. Results for analysis of a DU (Z11051).	11
Table 5.2. Results for the analysis of an HEU (Z11050) A solution, from the FY 2021 fission spectrum irradiation (R $\pm 1\sigma\%$) compared to ENDF values.	13

Table 5.3.	Atoms per fission of ^{237}U and ^{239}Np in DU (Z11051) and HEU (Z11050) A solution for the FY 2021 irradiation (N/f $\pm 1\sigma\%$).....	15
Table 5.4.	Summary of chemical yields following chemical separations for the in FY 2021 (Percent Yield $\pm \%$ RSD).....	16
Table 6.1.	Strontium-89 R-values for DU and HEU samples irradiated on the Flattop critical assembly compared to previous R-value campaigns and ENDF (R $\pm 1\sigma\%$).....	18
Table 6.2.	Yttrium-91 R-values for DU and HEU samples irradiated on the Flattop critical assembly compared to previous R-value campaigns and ENDF (R $\pm 1\sigma\%$).....	20
Table 6.3.	Relative and Absolute CFY for ^{91}Y	20
Table 6.4.	Zirconium-95 R-values for DU and HEU samples irradiated on the Flattop critical assembly compared to previous R-value campaigns and ENDF (R $\pm 1\sigma\%$).....	21
Table 6.5.	Zirconium-97 R-values for DU and HEU samples irradiated on the Flattop critical assembly compared to previous R-value campaigns and ENDF (R $\pm 1\sigma\%$).....	22
Table 6.6.	Ruthenium-103 R-values for DU and HEU samples irradiated on the Flattop critical assembly compared to previous R-value campaigns and ENDF (R $\pm 1\sigma\%$).....	23
Table 6.7.	Silver-111 R-values for DU and HEU samples irradiated on the Flattop critical assembly compared to previous R-value campaigns and ENDF (R $\pm 1\sigma\%$).....	24
Table 6.8.	Cadmium-115 R-values for DU and HEU samples irradiated on the Flattop critical assembly compared to previous R-value campaigns and ENDF V.III.0 (R $\pm 1\sigma\%$).....	25
Table 6.9.	Cadmium-115m R-values for DU and HEU samples irradiated on the Flattop critical assembly compared to previous R-value campaigns and JEFF3.1.1 (R $\pm 1\sigma\%$).....	26
Table 6.10.	Tellurium-132 R-values for DU and HEU samples irradiated on the Flattop critical assembly compared to previous R-value campaigns and ENDF (R $\pm 1\sigma\%$).....	27
Table 6.11.	Cesium-136 R-values for DU and HEU samples irradiated on the Flattop critical assembly compared to previous R-value campaigns and ENDF (R $\pm 1\sigma\%$).....	29
Table 6.12.	Cesium-137 R-values for DU and HEU samples irradiated on the Flattop critical assembly compared to previous R-value campaigns and ENDF (R $\pm 1\sigma\%$).....	29
Table 6.13.	Barium-140 R-values for DU and HEU samples irradiated on the Flattop critical assembly compared to previous R-value campaigns and ENDF (R $\pm 1\sigma\%$).....	31
Table 6.14.	Cerium-141 R-values for DU and HEU samples irradiated on the Flattop critical assembly compared to previous R-value campaigns and ENDF (R $\pm 1\sigma\%$).....	32

Table 6.15. Cerium-143 R-values for DU and HEU samples irradiated on the Flattop critical assembly compared to previous R-value campaigns and ENDF (R $\pm 1\sigma\%$).	33
Table 6.16. Cerium-144 R-values for DU and HEU samples irradiated on the Flattop critical assembly compared to previous R-value campaigns and ENDF (R $\pm 1\sigma\%$).	34
Table 6.17. Neodymium-147 R-values for DU sample irradiated on the Flattop critical assembly compared to previous R-value campaigns and ENDF (R $\pm 1\sigma\%$).	35
Table 6.18. Samarium-153 R-values for DU sample irradiated on the Flattop critical assembly compared to previous R-value campaigns and ENDF (R $\pm 1\sigma\%$).	36
Table 6.19. Europium-156 R-values for DU sample irradiated on the Flattop critical assembly compared to previous R-value campaigns and ENDF (R $\pm 1\sigma\%$).	37
Table 6.20. Terbium-161 R-values for DU and HEU samples irradiated on the Flattop critical assembly compared to previous R-value campaigns and ENDF (R $\pm 1\sigma\%$).	38
Table 9.1. Calculated literature R-values for select fission products. R-value and associated uncertainties were propagated from the fission yields of each fission product.	42

1.0 Introduction

Fission product yields and data are integral to the fundamental understanding of the fission process and feed directly into the nuclear forensics and nuclear physics models of the fission process. The stronger the foundation of the nuclear data is, whether that is the uncertainty associated with a decay path or the cumulative fission yield of a specific fission product, the stronger the conclusions that can be made from the models using these data.

Within the F2019 “Integral Measurements of Independent and Cumulative Fission Product Yields,” joint project (LA19-ML-Integral_Fission_Product_Yield-NDD3Ad), an area of particular focus has been the improvement of fission product yields as a function of incident neutron energy and target actinide using the capabilities reestablished and refined in previous years to support the nuclear forensics mission. This project addresses this nuclear data issue through a campaign of consistent and repeated measurements using the same neutron sources and experimental processes for each of the actinides investigated. Reducing uncertainties in fission product yields aids in the constraint of the multiparameter models used by nuclear forensics in support of attribution.

The measured fission product R-values (fission yields relative to ^{99}Mo) and spectral index using the ratio of fissions from the two targets, (^{238}U and ^{235}U targets) are presented for the two sources irradiated during the FY 2021 experimental campaign. Targets were prepared by Los Alamos National Laboratory (LANL) and irradiated on the Flattop critical assembly at the National Criticality Experiments Research Center (NCERC) located within the Device Assembly Facility (DAF). Details on the target manufacturing process can be found in a separate joint report (Uhnak et al. 2021a).

Comparisons were made between historical and current Pacific Northwest National Laboratory (PNNL) and LANL results, as well as literature values. Included in these comparisons were the short-lived actinides ^{237}U and ^{239}Np , and the fission products ^{89}Sr , ^{91}Y , $^{95/97}\text{Zr}$, ^{99}Mo , ^{111}Ag , $^{115/115\text{m}}\text{Cd}$, $^{136/137}\text{Cs}$, ^{140}Ba , $^{141/143/144}\text{Ce}$, ^{147}Nd , ^{153}Sm , ^{156}Eu , and ^{161}Tb , which provided total atoms as well as the R-values. This report contains the data from FY 2021, the sixth NCERC irradiation of highly enriched uranium (HEU) and depleted uranium (DU) in which PNNL has participated. Previous irradiations and subsequent separation and analysis occurred in FY 2013, FY 2014, FY 2015, FY 2017, and FY 2018. Data from each of the previous campaigns will be compared to the FY 2021 data.

2.0 Irradiation of Prepared Targets

The multiple targets LANL made are referenced in Table 2.1 by the designations assigned by LANL and PNNL. This report will only discuss targets shared between LANL and PNNL, and PNNL naming designations will be used to prevent confusion. Isotopic composition of the targets can be found in Table 2.2.

Table 2.1. Details on target including naming, mass, material, irradiation conditions, and dates.

Sample	Z11051	Z11050
Irradiation time (D)	0.0951	0.0951
Target mass (g)	0.3751	0.1830
Target material	DU	HEU
LANL name	4510	4511
Irradiation date	4/12/21	4/12/21
PNNL receipt date	4/20/21	4/20/21

DU = depleted uranium; HEU = highly enriched uranium; LANL = Los Alamos National Laboratory; PNNL = Pacific National Laboratory

Table 2.2. Isotopic composition in percent of the target materials. Further information on the target materials can be found in Uhnak et al. (2021a).

Target Material	Isotope							
	234	± (%)	235	± (%)	236	± (%)	238	± (%)
DU	7.81E-04	6.2	2.00E-01	N/A	2.76E-03	5.3	99.8	0.71
HEU	1.1239	0.38	93.236	0.01	0.2592	0.62	5.381	0.28

DU = depleted uranium; HEU = highly enriched uranium; N/A = not applicable

2.1 Preparation of A Solution and Splits

Targets were dissolved using the methods described in the joint report (Uhnak et al. 2021a), producing the A solutions in 4 M HNO₃. The details of the A solution splits obtained from LANL are included in Table 2.3. PNNL received more than 50 percent of the total A solution mass for sample Z11051, but less than 50 percent of the A solution for Z11050. To provide a uniform interlaboratory comparison, the grams of target per gram of A solution value is included (g target/ g A). This value is used to relate fission product data directly back to the target mass rather than the A solution mass.

Table 2.3. A solution splits sent to PNNL.

Sample	Z11051	Z11050
Total mass A solution (g)	36.4209	52.5868
g target/g A	0.01030	0.00348
PNNL split (g A solution)	23.1107	22.6838

PNNL = Pacific National Laboratory

3.0 Radiochemical Methodology

3.1 Radiochemical Processing at PNNL

3.1.1 Sample Splitting and Spiking

The PNNL A solutions were split according to the masses shown in Table 3.1, included along with this is the percent of the PNNL A solutions, the mass of U in these fractions, and the number of fissions relative to thermal ^{99}Mo . Table 3.2 shows the tracer additions for the stable and radioactive yield tracers used. Due to the number of fissions in these samples, it was determined that it would be better if the samples were split into thirds to provide enough activity for adequate statistics on the various fission products in each PNNL A solution or separated fraction. The chemistry replicates moved on to the separations discussed below in detail, while the whole solution gamma energy analysis (GEA) was rotated among several detectors for analysis.

Table 3.1. PNNL A solution splits.

DU Target (Z11051)				
	Mass of A solution (g)	Percent of A solution	Mass of U* (mg)	Fissions Thermal $^{99}\text{Mo}^*$
Whole Solution GEA	7.4190	31.5%	0.075	$2.00 \times 10^{11} \pm 1.7\%$
Chemistry Rep 1	8.0593	34.3%	0.082	$2.17 \times 10^{11} \pm 1.7\%$
Chemistry Rep 2	8.0759	34.2%	0.081	$2.17 \times 10^{11} \pm 1.7\%$
HEU Target (Z11050)				
	Mass of A solution (g)	Percent of A solution	Mass of U* (mg)	Fissions Thermal $^{99}\text{Mo}^*$
Whole Solution GEA	7.5214	32.5%	0.026	$4.61 \times 10^{11} \pm 1.6\%$
Chemistry Rep 1	7.7913	33.7%	0.027	$4.78 \times 10^{11} \pm 1.6\%$
Chemistry Rep 2	7.7964	33.7%	0.027	$4.78 \times 10^{11} \pm 1.6\%$

*Based on PNNL GEA analysis of A solution
DU = depleted uranium; GEA = gamma energy analysis; HEU = highly enriched uranium

Table 3.2. Tracer spiking for Z11051 and Z11050 for the tracers ^{237}Np , $^{110\text{m}}\text{Ag}$, ^{109}Cd , ^{134}Cs , ^{152}Eu and stable tracers Sm, Eu, Tb, Y, and Sr. These quantities were also included in the tracer blank.

Target	HEU	DU
Z#	Z11050	Z11051
^{237}Np (Bq)	370	370
$^{110\text{m}}\text{Ag}$ (Bq)	370	370
Gamma: ^{109}Cd (Bq)	3700	3700
^{134}Cs , ^{152}Eu (Bq)	370	370
CC1: Sm, Eu, Tb (μg)	100	100
Sr (μg)	50	50
Y (pg)	150	150

3.1.2 Analysis of A Solution

The aliquot labeled “Whole Solution GEA” in Table 3.1 for Z11051 and Z11050 was analyzed by GEA to quantify the peak yield fission products. These samples were in a calibrated geometry consisting of a 10 mL solution volume within a 20 mL poly scintillation vial. The GEA results were decay-corrected to the end of bombardment. Each of the A solutions was analyzed multiple times, on multiple detectors; dates of these analyses are included in Table 3.3. The short 30-minute screening count was included in the analysis with little difference in the counting statistics or detected analytes when excluding the initial screen count. The count used for each analyte is included in Table 3.4.

All analytes determined from GEA counts were the result of at least two individual counts. The use of Compton suppression GEA was not possible for this exercise. This was due to an effort to increase the number of fissions in the replicate samples processed through chemistry. A single A solution sample was provided for both the GEA and Compton suppression analysis. This A solution sample was just above the activity suitable for the analysis methods. Therefore, the results are not reported; but the historical results are included in Section 6.0.

Table 3.3. Dates for each GEA of A solutions for samples Z11050 and Z11051.

Count	Z11051	Z11050
1	4/20/21*	4/20/21*
2	4/20/21	4/20/21
3	4/21/21	4/21/21
4	4/23/21	4/23/21
5	4/24/21	4/24/21
6	4/25/21	4/25/21
7	4/29/21	4/29/21
8	5/5/21	5/5/21
9	5/11/21	5/11/21

*Short 30-minute screening count

Table 3.4. PNNL A solution GEA used to quantify applicable radionuclides. Values correspond to the count numbers in Table 3.3.

Isotope	Z11051	Z11050	Isotope	Z11051	Z11050
⁹¹ Sr	N/A	N/A	¹³⁷ Cs	5-9	8-9
⁹¹ Y	5,8,9	7-9	¹⁴⁰ Ba	2-9	1-9
⁹⁵ Zr	1-9	1-9	¹⁴¹ Ce	1-9	1-9
⁹⁷ Zr	1-4	1-3	¹⁴³ Ce	1-6	1-7
⁹⁹ Mo	3-7	1-8	¹⁴⁴ Ce	4-9	7-9
¹⁰³ Ru	2-9	1-9	¹⁴⁷ Nd	1,3-5,8,9	1-9
¹¹¹ Ag	7,8	2,6,9	¹⁵⁶ Eu	5,7-9	N/A
¹¹² Ag	N/A	2	²³⁵ U	5-8	3-9
¹¹⁵ Cd	2-4	1-4	²³⁷ U	1-6,8,9	2.4-6,8
¹³² Te	2-4,9	1-9	²³⁸ U	3,9	N/A
¹³⁶ Cs	N/A	2-7	²³⁹ Np	1-6,8,9	1-6,9

3.2 Radiochemical Separations

3.2.1 Separation Chemistry Methodology and Discussion

Separation chemistry was similar to previous campaigns with some notable changes, most similar to the methods presented in Uhnak et al. (2021b). Due to the mass of the targets, deliberation of the starting chemistry was necessary. The mass of the DU target was close to exceeding the method developed in previous campaigns using two UTEVA resin cartridges, but the mass of the HEU target was below what would necessitate a 25 mL UTEVA column. To simplify reagent preparation and maintain a “apples-to-apples” comparison the 25 mL UTEVA column was used for both targets. The full chemistry separation scheme is shown in Figure 3.1.

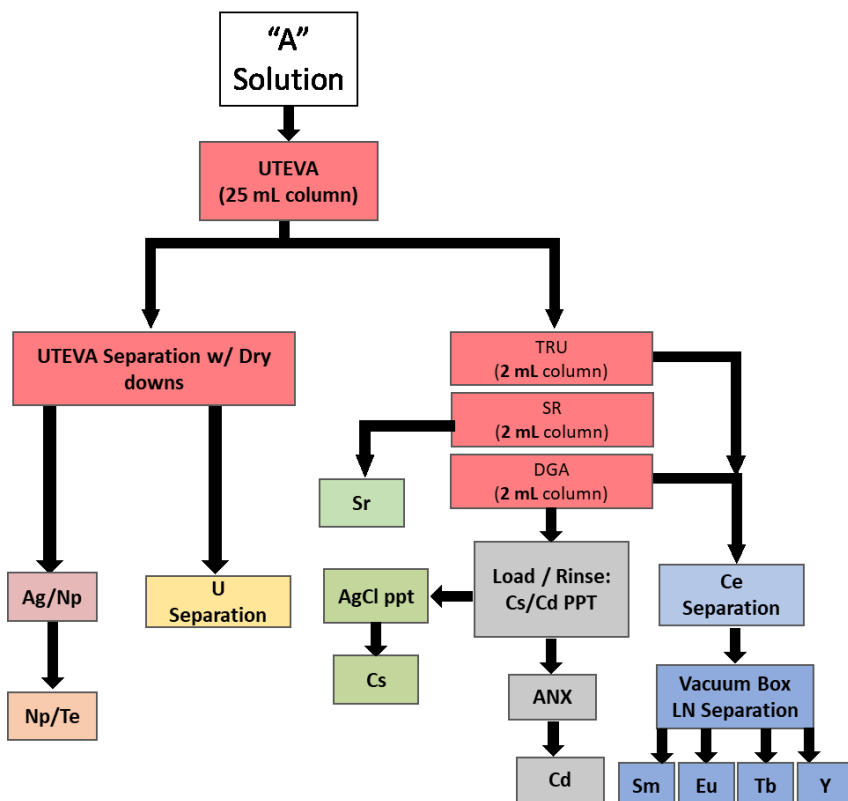


Figure 3.1. Radiochemical processing scheme at PNNL for dissolved A solutions of irradiated U target in FY 2021, process used for both DU and HEU targets.

The chemistry used downstream from the initial separation was identical to previous campaigns from FY 2020, except for the use of a vacuum box separation for the rare earth fission products (Sm, Eu, Tb, and Y), and the several small changes described below along with the results of these changes. This process was developed by collaborators in the United Kingdom at the Atomic Weapons Establishment and is being optimized under another project.

- U elution was accomplished with 100 mL 0.1 M HEDTA, 0.25 M ammonium citrate.
 - U fraction was screened for the presence of radiotellurium by GEA to determine if a spontaneous deposition on Ag discs was necessary to remove the Te.
 - It was determined in other but similar work that the presence of Ag causes issues with the analysis of U by kinetic phosphorescence analysis (KPA).

- The U fraction was clean of all other radioisotopes.
- The Te found was in a separated fraction alone.
- A separate Mo fraction was also isolated without contamination.
- Ce isolation was not accomplished as planned due to the date of preparation of the NaBrO₃ reagent. The oxidative ability of the reagent was not sufficient to oxidize the Ce.
 - The Ce data reported below in Section 5.0 are from the load and rinse fraction coming off of the DGA resin column. In future efforts the NaBrO₃ will be made within hours of the Ce separation.
- The rare earth separation was accomplished using Eichrom LN resin cartridges attached to a vacuum box. The elution conditions are shown in Table 3.5.

Table 3.5. Elution conditions for the separation of rare earth fission products on vacuum box.

Fraction Number	Eluent (HNO ₃)	Volume (mL)	Predicted Fractions
	0.1 (load)	1	
	0.1	4 X 1 mL rinses	
2	0.3	35	Nd/Am
3	0.3	35	Sm
4	0.3	10	Waste (Sm/Eu)
5	0.75	10	Eu
6	0.75	10	Waste (Eu)
7	2	10	Tb
8	4	15	Y

- Each of the fractions including those expected to be waste fractions were analyzed by GEA to determine the level of contamination in each fraction. The level of contamination can be seen in Figure 3.2. The HEU target was selected for this comparison, as this was less pure than the DU target. Percent yields used in this figure were calculated relative to the initial atoms/g determined in the A solution (where applicable).
 - Fraction 1 contains the lightest lanthanides and Ba.
 - Fraction 2 contains the Nd and the Pm, with a small quantity of ¹⁴⁰La present. This is also expected to contain Am when present.
 - Fraction 3 contains a highly pure Sm fraction. This is of particular importance as the detection of ¹⁵³Sm requires high purity due to the gamma emission energy and branching ratio.
 - Fractions 4 and 6 are “waste” fractions, intended to provide a buffer between the elution conditions used for Sm and Eu, thus decreasing the potential for cross contamination among the Sm, Eu, and Tb fractions.
 - Fraction 7, the Tb fraction contained only ¹⁶¹Tb. This is not surprising as this fraction goes through another supplemental cleanup column, though the recovery of Tb was about 100%.
 - Fraction 8, the Y fraction, contained all Y as well as a small quantity of the residual lanthanides, like Eu and Tb.

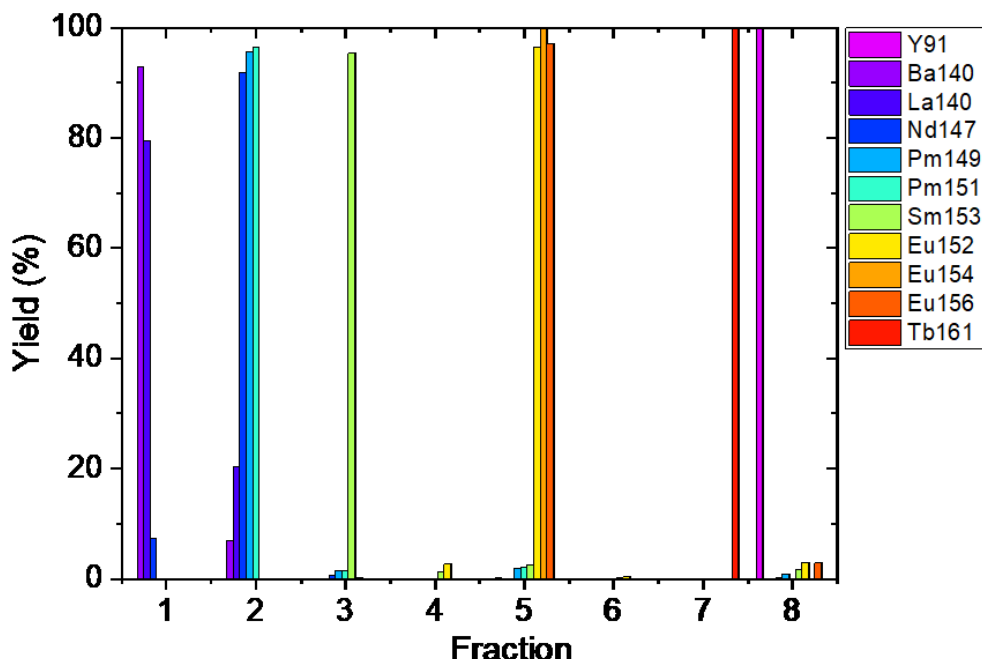


Figure 3.2. Relative percent yield of each lanthanide fraction collected found in the HEU target.

Using this method for the lanthanide fission product separation decreased the time frame required to isolate the Sm, Eu, Tb, and Y fractions by more than twofold, relative to the method used in FY 2020 (Uhnak et al. 2021b).

3.2.2 Analysis of Separated Fractions

All analysis was conducted on both replicates from both the Z11051 and Z11050 A solutions along with the tracer and reagent blanks. Separated fractions and A solution aliquots were analyzed by GEA using calibrated geometry (i.e., 10 mL in a 20 mL poly vial). Data from GEA were processed using Genie 2000 software (Canberra Industries 2006). The Cs fractions were analyzed using 100 mL of solution in either a 150 mL or 250 mL high-density polyethylene bottle. Strontium was analyzed using thermal ionization mass spectrometry (TIMS). Terbium was analyzed by low energy photon spectroscopy (LEPS). Uranium concentration was determined using both GEA, as well as KPA. The KPA was a Chemcheek Model 11 using KPAwin version 1.2.9.

Corrections for yield determination following the separations were made for the radiotracers of ^{109}Cd , $^{110\text{m}}\text{Ag}$, ^{134}Cs , and ^{152}Eu using analysis by GEA. Stable tracers (Sr, Sm, Eu, Tb, and Y) were made for the analysis by inductively coupled plasma optical emission spectroscopy (ICP-OES). Separated U fractions were analyzed by GEA and KPA. Strontium was analyzed by TIMS, with the yield determined using inductively coupled plasma optical emission spectroscopy (ICP-OES)—used for determination of the efficacy of the chemical separation.

Yttrium was analyzed by both ICP-OES as well as inductively coupled plasma mass spectrometry (ICP-MS). Presence of Y in the reagent blank indicated an unaccounted-for

source of Y in the chemistry at levels about 12% of the Y tracer concentration. The data were background-corrected to account for this issue and will be further investigated to determine the source.

4.0 R-value Calculation

The analytical results were used to calculate the R-value for each fission product; the method for calculating the R-value is shown in **Error! Reference source not found.** PNNL has a running historical r-value (r_{hist}) for each isotope, based on the results from the last five thermal calibration (t-cal) exercises where available. A t-cal exercise involves the thermal irradiation of ^{235}U followed by separation and radiometric analysis. The historical r-value replaces the Evaluated Nuclear Data File (ENDF)/B-VIII.0 cumulative fission yield (CFY) in the R-value calculation. The historical r-values used in the R-value calculation are shown in Table 4.1. A few isotopes including ^{91}Sr , ^{93}Y , ^{112}Ag , and ^{156}Sm are not measured in t-cal solutions and do not have r_{hist} values; in these cases, the applicable ENDF/B-VIII.0 CFY values have been used.

$$R = \frac{\left(\frac{N_X}{N_{Mo99}}\right)_{Measured}}{\left(\frac{N_X}{N_{Mo99}}\right)_{U235\ Thermal}} = \frac{\left(\frac{N_X}{N_{Mo99}}\right)_{Measured}}{\left(\frac{CFY_X}{CFY_{Mo99}}\right)_{U235\ Thermal}} = \frac{\left(\frac{N_X}{N_{Mo99}}\right)_{Measured}}{r_{hist}} \quad \text{Eq.1}$$

Where

N_X = atoms of isotope X per gram of A solution

N_{Mo99} = atoms of ^{99}Mo per gram of A solution

CFY_X = cumulative fission yield for isotope X for ^{235}U thermal fission

CFY_{Mo99} = cumulative fission yield for ^{99}Mo for ^{235}U thermal fission

r_{hist} = historical r-value as determined in Eq. 2

$$r_{hist} = \left(\frac{N_X}{N_{Mo99}}\right)_{t-cal} \quad \text{Eq.2}$$

Where

N_X = atoms of isotope X per gram of A solution in a t-cal sample

N_{Mo99} = atoms of ^{99}Mo per gram of A solution in a t-cal sample

t-cal = thermal calibration exercise sample

Table 4.1. PNNL historical r-values.

Isotope	r_{hist}	Isotope	r_{hist}
^{89}Sr	0.793	^{136}Cs	9.67×10^{-4}
^{91}Sr	N/A	^{137}Cs	1.05
^{91}Y	0.939	^{140}Ba	1.05
^{93}Y	N/A	^{141}Ce	0.971
^{95}Zr	1.09	^{143}Ce	0.994
^{97}Zr	1.05	^{144}Ce	0.910
^{103}Ru	0.504	^{147}Nd	0.365
^{111}Ag	2.80×10^{-3}	^{153}Sm	2.22×10^{-2}
^{112}Ag	N/A	^{156}Sm	N/A
$^{115}\text{Cd}^*$	2.21×10^{-3}	^{155}Eu	5.37×10^{-3}
^{115m}Cd	7.90×10^{-5}	^{156}Eu	2.44×10^{-3}
^{132}Te	0.719	^{161}Tb	1.29×10^{-5}

Isotope	r_{hist}	Isotope	r_{hist}
*Recent work on ^{115}Cd , for another project, revealed errors in software that have been fixed, which consequently adjusted the ^{109}Cd analysis.			

5.0 Summary of FY 2021 Results

A summary of the FY 2021 results has been compiled for the A solutions including U concentration, masses, fissions, results with comparisons to ENDF/B-VII.I (Chadwick et al. 2011) and with historical data from FY 2013, FY 2014, FY 2015, FY 2017, and FY 2018 for both DU and HEU. The results from the analysis of separated fractions for the FY 2021 irradiation are included in Table 5.1 and Table 5.2, for Z11051 and Z11050 respectively. Table 5.3 contains the data for the short-lived actinides for both Z11051 and Z11050. The ENDF R-values have been calculated using the ENDF/B-VII.I CFY for ^{235}U thermal, ^{235}U fission spectrum, and ^{238}U fission spectrum. A more detailed discussion of individual analytes with comparisons with prior measurements is presented in Section 0.

Table 5.1. Results for analysis of a DU (Z11051) A solution and separated fractions from the FY 2021 fission spectrum irradiation ($R \pm 1\sigma$) compared to ENDF values. Results include atoms/g, R values, ENDF R, Chemical yields, and analysis methods. Values in bold and italics are the atoms/g for the mass of the initial target prepared by LANL.

Isotope	Atoms/g A (Atoms/g target)	R DU	R ENDF - ^{238}U Fission Spectrum	Chemical Yield (%)	Method
^{89}Sr	$7.13 \times 10^8 \pm 0.9\%$ $(7.13 \times 10^{10} \pm 0.9\%)$	$0.555 \pm 2.77\%$	$0.578 \pm 2.62\%$	96.0%	Separated Fraction (TIMS)
^{91}Sr	N/A	N/A	$0.686 \pm 2.99\%$	N/A	N/A
^{91}Y	$1.03 \times 10^9 \pm 44.9\%$ $(1.03 \times 10^{11} \pm 44.9\%)$	$0.621 \pm 44.9\%$	$0.686 \pm 90.5\%$	N/A	A Solution (GEA)
	$8.77 \times 10^8 \pm 5.42\%$ $(8.77 \times 10^{10} \pm 5.42\%)$	$0.563 \pm 5.53\%$		90.0%	Separated Fraction(OES)*
	$9.01 \times 10^8 \pm 4.32\%$ $(9.01 \times 10^{10} \pm 4.32\%)$	$0.578 \pm 4.46\%$		97.1%	Separated Fraction(MS)*
^{93}Y	N/A	N/A	$0.764 \pm 90.5\%$	N/A	N/A
^{95}Zr	$1.36 \times 10^9 \pm 2.00\%$ $(1.36 \times 10^{11} \pm 2.00\%)$	$0.753 \pm 2.83\%$	$0.783 \pm 2.80\%$	N/A	A Solution (GEA)
^{97}Zr	$1.57 \times 10^9 \pm 2.66\%$ $(1.57 \times 10^{11} \pm 2.66\%)$	$0.901 \pm 3.33\%$	$0.921 \pm 3.14\%$	N/A	A Solution (GEA)
^{99}Mo	$1.66 \times 10^9 \pm 2.00\%$ $(1.66 \times 10^{11} \pm 2.00\%)$	N/A	N/A	N/A	A Solution (GEA)
^{103}Ru	$1.60 \times 10^9 \pm 2.27\%$ $(1.60 \times 10^{11} \pm 2.27\%)$	$1.92 \pm 3.02\%$	$2.05 \pm 2.80\%$	N/A	A Solution (GEA)
^{111}Ag	$2.29 \times 10^7 \pm 20.4\%$ $(2.29 \times 10^9 \pm 20.4\%)$	$4.93 \pm 20.5\%$	$4.05 \pm 4.89\%$	N/A	A Solution (GEA)
	$1.84 \times 10^7 \pm 3.30\%$ $(1.84 \times 10^9 \pm 3.30\%)$	$3.95 \pm 3.85\%$		85.3%	Separated Fraction
^{112}Ag	N/A	N/A	$4.25 \pm 7.48\%$	N/A	N/A
^{115}Cd	$9.89 \times 10^6 \pm 28.7\%$ $(9.89 \times 10^8 \pm 28.7\%)$	$2.70 \pm 28.7\%$	$2.95 \pm 6.63\%$	N/A	A Solution (GEA)
	$1.11 \times 10^7 \pm 2.44\%$ $(1.11 \times 10^9 \pm 2.44\%)$	$3.03 \pm 4.03\%$		82.0%	Separated Fraction (GEA)

Table 5.1. (contd.)

Isotope	Atoms/g A (Atoms/g target)	R DU	R ENDF - ^{238}U Fission Spectrum	Chemical Yield (%)	Method
^{115m}Cd	$1.07 \times 10^6 \pm 32.9\%$ $(1.07 \times 10^8 \pm 32.9\%)$	$8.17 \pm 38.5\%$	$3.07 \pm 8.71\% \ddagger$	82.0%	Separated Fraction (GEA)
^{132}Te	$1.36 \times 10^9 \pm 2.74\%$ $(1.36 \times 10^{11} \pm 2.74\%)$	$1.14 \pm 3.40\%$	$1.18 \pm 2.80\%$	N/A	A Solution (GEA)
^{136}Cs	N/A	N/A	$0.172 \pm 90.5\%$	N/A	A Solution (GEA)
	$1.44 \times 10^5 \pm 13.1\%$ $(1.44 \times 10^7 \pm 13.1\%)$	$0.09 \pm 13.5\%$		96.9%	Separated Fraction (GEA)
^{137}Cs	$1.61 \times 10^9 \pm 6.79\%$ $(1.61 \times 10^{11} \pm 6.79\%)$	$0.923 \pm 7.08\%$	$0.969 \pm 2.27\%$	N/A	A Solution (GEA)
	$1.50 \times 10^9 \pm 3.66\%$ $(1.50 \times 10^{11} \pm 3.66\%)$	$0.859 \pm 4.62\%$		96.9%	Separated Fraction (GEA)
^{140}Ba	$1.57 \times 10^9 \pm 2.53\%$ $(1.57 \times 10^{11} \pm 2.53\%)$	$0.901 \pm 3.32\%$	$0.927 \pm 2.33\%$	N/A	A Solution (GEA)
^{141}Ce	$1.33 \times 10^9 \pm 3.39\%$ $(1.33 \times 10^{11} \pm 3.39\%)$	$0.823 \pm 3.94\%$	$0.904 \pm 3.57\%$	N/A	A Solution (GEA)
^{143}Ce	$1.24 \times 10^9 \pm 3.89\%$ $(1.24 \times 10^{11} \pm 3.89\%)$	$0.750 \pm 4.37\%$	$0.769 \pm 2.80\%$	N/A	A Solution (GEA)
^{144}Ce	$1.09 \times 10^9 \pm 8.49\%$ $(1.09 \times 10^{11} \pm 8.49\%)$	$0.722 \pm 8.72\%$	$0.819 \pm 2.52\%$	N/A	A Solution (GEA)
	$1.20 \times 10^9 \pm 4.10\%$ $(1.20 \times 10^{11} \pm 4.10\%)$	$0.795 \pm 5.15\%$		88.8%	Separated Fraction
^{147}Nd	$6.76 \times 10^8 \pm 2.85\%$ $(6.76 \times 10^{10} \pm 2.85\%)$	$1.12 \pm 3.48\%$	$1.14 \pm 2.80\%$	N/A	A Solution (GEA)
^{153}Sm	$8.42 \times 10^7 \pm 3.01\%$ $(8.42 \times 10^9 \pm 3.01\%)$	$2.29 \pm 3.62\%$	$2.60 \pm 4.89\%$	84.2%	Separated Fraction
^{155}Eu	$4.19 \times 10^7 \pm 8.49\%$ $(4.19 \times 10^9 \pm 8.49\%)$	$4.70 \pm 8.72\%$	$4.36 \pm 16.6\%$	93.1%	Separated Fraction (GEA)
	$4.08 \times 10^7 \pm 8.47\%$ $(4.08 \times 10^9 \pm 8.47\%)$	$4.58 \pm 9.62\%$		95.7%	Separated Fraction (OES)
^{156}Eu	$1.64 \times 10^7 \pm 12.3\%$ $(1.64 \times 10^9 \pm 12.3\%)$	$4.08 \pm 12.5\%$	$5.07 \pm 4.89\%$	N/A	A Solution (GEA)
	$1.81 \times 10^7 \pm 5.08\%$ $(1.81 \times 10^9 \pm 5.08\%)$	$4.48 \pm 5.46\%$		93.1%	Separated Fraction (GEA)
	$1.76 \times 10^7 \pm 5.08\%$ $(1.76 \times 10^9 \pm 5.08\%)$	$4.36 \pm 5.46\%$		95.7%	Separated Fraction (OES)
^{161}Tb	$2.45 \times 10^5 \pm 5.22\%$ $(2.45 \times 10^7 \pm 5.22\%)$	$11.5 \pm 5.59\%$	$14.1 \pm 5.27\%$	101% [†]	Separated Fraction

Table 5.1. (contd.)

Isotope	Atoms/g A (Atoms/g target)	Chemical Yield (%)	Method
U	N/A	57.2%	Separated Fraction (KPA)
²³⁵ U	$3.29 \times 10^{16} \pm 2.80\%$ <i>($3.29 \times 10^{18} \pm 2.80\%$)</i>	57.7%	Separated Fraction (GEA of ²³⁵ U)
²³⁷ U	$1.28 \times 10^9 \pm 3.30\%$ <i>($1.28 \times 10^{11} \pm 3.30\%$)</i>	57.7%	Separated Fraction
²³⁹ Np	$1.50 \times 10^{10} \pm 5.69\%$ <i>($1.50 \times 10^{12} \pm 5.69\%$)</i>	81.5%	Separated Fraction (GEA)

* Chemical yielding issues present; ‡ Likely requires updates to nuclear data; † Has $\pm 2.5\%$ uncertainty in the yield
DU = depleted uranium; ENDF = Evaluated Nuclear Data File; GEA = gamma energy analysis; KPA = kinetic phosphorescence analysis; MS = mass spectrometer; N/A = not applicable, OES = optical emission spectroscopy; TIMS = thermal ionization mass spectrometry

Table 5.2. Results for the analysis of an HEU (Z11050) A solution, from the FY 2021 fission spectrum irradiation ($R \pm 1\sigma\%$) compared to ENDF values. Results include atoms/g, R values, ENDF R, Chemical yields, and analysis methods. Values in bold and italics are the atoms/g for the mass of the initial target prepared by LANL.

Isotope	Atoms/g A (Atoms/g target)	R HEU	R ENDF - ²³⁵ U Fission Spectrum	Chemical Yield (%)	Method
⁸⁹ Sr	$2.55 \times 10^9 \pm 0.89\%$ <i>($7.28 \times 10^{11} \pm 0.9\%$)</i>	$0.902 \pm 2.87\%$	$0.950 \pm 2.62\%$	92.8%	Separated Fraction (TIMS)
⁹¹ Sr	N/A	N/A	$1.01 \pm 2.99\%$	N/A	N/A
⁹¹ Y	$3.06 \times 10^9 \pm 12.2\%$ <i>($8.73 \times 10^{12} \pm 12.2\%$)</i>	$0.839 \pm 12.4\%$	$1.01 \pm 90.5\%$	N/A	A Solution (GEA)
	$3.18 \times 10^9 \pm 5.43\%$ <i>($9.10 \times 10^{12} \pm 5.43\%$)</i>	$0.931 \pm 5.83\%$		55.2%	Separated Fraction(OES)*
	$3.27 \times 10^9 \pm 4.25\%$ <i>($9.34 \times 10^{12} \pm 4.25\%$)</i>	$0.897 \pm 4.25\%$		59.1%	Separated Fraction(MS)*
⁹³ Y	N/A	N/A	$1.01 \pm 90.5\%$	N/A	N/A
⁹⁵ Zr	$3.79 \times 10^9 \pm 2.00\%$ <i>($1.08 \times 10^{12} \pm 2.00\%$)</i>	$0.954 \pm 2.91\%$	$1.02 \pm 2.62\%$	N/A	A Solution (GEA)
⁹⁷ Zr	$3.63 \times 10^9 \pm 2.30\%$ <i>($1.04 \times 10^{12} \pm 2.30\%$)</i>	$0.949 \pm 3.13\%$	$1.03 \pm 3.14\%$	N/A	A Solution (GEA)
⁹⁹ Mo	$3.64 \times 10^9 \pm 2.12\%$ <i>($1.04 \times 10^{12} \pm 2.12\%$)</i>	N/A	N/A	N/A	A Solution (GEA)
¹⁰³ Ru	$1.95 \times 10^9 \pm 2.00\%$ <i>($5.56 \times 10^{11} \pm 2.00\%$)</i>	$1.06 \pm 2.91\%$	$1.10 \pm 2.80\%$	N/A	A Solution (GEA)
¹¹¹ Ag	$2.82 \times 10^7 \pm 13.8\%$ <i>($8.04 \times 10^9 \pm 13.8\%$)</i>	$2.76 \pm 13.95\%$	$2.51 \pm 5.27\%$	N/A	A Solution (GEA)
	$2.77 \times 10^7 \pm 3.30\%$ <i>($7.90 \times 10^9 \pm 3.30\%$)</i>	$2.71 \pm 4.40\%$		89.7%	Separated Fraction

Table 5.2. (contd.)

Isotope	Atoms/g A (Atoms/g target)	R HEU	R ENDF - ^{235}U Fission Spectrum	Chemical Yield (%)	Method
^{112}Ag	N/A	N/A	$2.97 \pm 6.91\%$	N/A	A Solution (GEA)
^{115}Cd	$1.98 \times 10^7 \pm 4.97\%$ $(5.67 \times 10^9 \pm 4.97\%)$	$2.46 \pm 5.40\%$	$2.76 \pm 6.91\%$	N/A	A Solution (GEA)
	$2.47 \times 10^7 \pm 2.40\%$ $(7.05 \times 10^9 \pm 2.40\%)$	$3.06 \pm 4.06\%$		75.8%	Separated Fraction (GEA)
^{115m}Cd	$9.06 \times 10^5 \pm 27.5\%$ $(2.59 \times 10^9 \pm 27.5\%)$	$3.15 \pm 33.9\%$	$2.86 \pm 23.85\% \ddagger$	75.8%	Separated Fraction (GEA)
^{132}Te	$2.83 \times 10^9 \pm 2.31\%$ $(8.08 \times 10^{11} \pm 2.31\%)$	$1.08 \pm 3.13\%$	$1.12 \pm 3.14\%$	N/A	A Solution (GEA)
^{136}Cs	$8.44 \times 10^6 \pm 5.57\%$ $(2.41 \times 10^9 \pm 5.57\%)$	$2.40 \pm 5.96\%$	$2.18 \pm 90.5\%$	N/A	A Solution (GEA)
	$7.65 \times 10^6 \pm 2.00\%$ $(2.19 \times 10^9 \pm 2.00\%)$	$2.17 \pm 3.84\%$		94.3%	Separated Fraction
^{137}Cs	$3.87 \times 10^9 \pm 3.26\%$ $(1.10 \times 10^{12} \pm 3.26\%)$	$1.01 \pm 3.89\%$	$1.03 \pm 2.10\%$	N/A	A Solution (GEA)
	$3.78 \times 10^9 \pm 2.00\%$ $(1.08 \times 10^{12} \pm 2.00\%)$	$0.988 \pm 3.34\%$		94.3%	Separated Fraction (GEA)
^{140}Ba	$3.55 \times 10^9 \pm 2.00\%$ $(1.01 \times 10^{12} \pm 2.00\%)$	$0.927 \pm 2.91\%$	$0.989 \pm 2.43\%$	N/A	A Solution (GEA)
^{141}Ce	$3.41 \times 10^9 \pm 6.65\%$ $(9.74 \times 10^{11} \pm 6.65\%)$	$0.963 \pm 6.98\%$	$1.05 \pm 3.57\%$	N/A	A Solution (GEA)
^{143}Ce	$3.28 \times 10^9 \pm 5.86\%$ $(9.36 \times 10^{11} \pm 5.86\%)$	$0.904 \pm 6.23\%$	$0.989 \pm 2.80\%$	N/A	A Solution (GEA)
^{144}Ce	$3.00 \times 10^9 \pm 11.2\%$ $(8.58 \times 10^{11} \pm 11.2\%)$	$0.906 \pm 11.4\%$	$0.985 \pm 2.52\%$	N/A	A Solution (GEA)
	$2.99 \times 10^9 \pm 7.02\%$ $(8.54 \times 10^{11} \pm 7.02\%)$	$0.902 \pm 7.72\%$		89.6%	Separated Fraction
^{147}Nd	$1.27 \times 10^9 \pm 2.23\%$ $(3.62 \times 10^{11} \pm 2.23\%)$	$0.952 \pm 3.07\%$	$1.14 \pm 2.80\%$	N/A	A Solution (GEA)
^{153}Sm	$8.98 \times 10^7 \pm 2.98\%$ $(2.56 \times 10^{10} \pm 2.98\%)$	$1.11 \pm 5.57\%$	$1.27 \pm 6.47\%$	83.0%	Separated Fraction
^{156}Eu	N/A	N/A	$1.40 \pm 4.89\%$	N/A	A Solution (GEA)
	$1.39 \times 10^7 \pm 4.66\%$ $(3.96 \times 10^9 \pm 4.66\%)$	$1.57 \pm 6.04\%$		85.8%	Separated Fraction (GEA)
	$1.35 \times 10^7 \pm 4.65\%$ $(3.85 \times 10^9 \pm 4.65\%)$	$1.52 \pm 5.11\%$		87.9%	Separated Fraction (OES)
^{161}Tb	$1.93 \times 10^5 \pm 4.44\%$ $(5.52 \times 10^7 \pm 4.4\%)$	$4.11 \pm 4.92\%$	$4.01 \pm 7.48\%$	80.5%	Separated Fraction

Table 5.2. (contd.)

Isotope	Atoms/g A (Atoms/g target)	Chemical Yield (%)	Method
U	N/A	90.4%	Separated Fraction (KPA)
^{235}U	$7.43 \times 10^{18} \pm 1.20\%$ $(2.12 \times 10^{20} \pm 1.20\%)$	86.7%	Separated Fraction (GEA)
^{237}U	$4.50 \times 10^7 \pm 2.87\%$ $(1.29 \times 10^{10} \pm 2.87\%)$	90.4%	Separated Fraction (KPA)
^{237}U	$4.48 \times 10^7 \pm 2.80\%$ $(1.28 \times 10^{10} \pm 2.80\%)$	86.7%	Separated Fraction (GEA)
^{239}Np	$2.53 \times 10^8 \pm 3.30\%$ $(7.22 \times 10^9 \pm 3.30\%)$	90.9%	Separated Fraction (GEA)

* Chemical yielding issues present; ‡ Likely requires updates to nuclear data

ENDF = Evaluated Nuclear Data File; HEU = highly enriched uranium; GEA = gamma energy analysis; KPA = kinetic phosphorescence analysis; MS = mass spectrometer; N/A = not applicable, OES = optical emission spectroscopy; TIMS = thermal ionization mass spectrometry.

Table 5.3. Atoms per fission of ^{237}U and ^{239}Np in DU (Z11051) and HEU (Z11050) A solution for the FY 2021 irradiation (N/f $\pm 1\sigma\%$).

Isotope		N/f	Measurement Method
DU (Z11051)	^{237}U	$4.71 \times 10^{-2} \pm 4.11\%$	Sep Fraction (GEA)
	^{239}Np	$0.553 \pm 5.69\%$	Sep Fraction (GEA)
	$^{237}\text{U}/^{239}\text{Np}$	$8.51 \times 10^{-2} \pm 7.02\%$	
HEU (Z11050)	^{237}U	$4.48 \times 10^{-4} \pm 3.78\%$	Sep Fraction (GEA)
	^{239}Np	$4.24 \times 10^{-3} \pm 4.10\%$	Sep Fraction (GEA)
	$^{237}\text{U}/^{239}\text{Np}$	$0.177 \pm 5.58\%$	

DU = depleted uranium; GEA = gamma energy analysis; HEU = highly enriched uranium

The chemical yields associated with measurement of the separated fractions of the DU and HEU A solutions are presented in Table 5.4. Aspects of processing that may have affected chemical yields for individual analytes are further discussed in Section 0 where results for each analyte are presented in detail.

Table 5.4. Summary of chemical yields following chemical separations for the in FY 2021 (Percent Yield \pm %RSD).

Isotope	DU	HEU	Yield Method (Tracer)
	Percent Yield \pm %RSD	Percent Yield \pm %RSD	
⁸⁹ Sr	96.0	92.8	ICP-OES (Stable Sr)
⁹¹ Y	90-97.1	55.2-59.1	ICP-OES/ICP-MS (Stable Y)
¹¹¹ Ag	85.3	89.7	GEA (^{110m} Ag)
¹¹⁵ Cd	82	75.8	GEA (¹⁰⁹ Cd)
^{115m} Cd	82	75.8	GEA (¹⁰⁹ Cd)
¹³⁶ Cs	96.9	94.3	GEA (¹³⁴ Cs)
¹³⁷ Cs	96.9	94.3	GEA (¹³⁴ Cs)
¹⁴⁴ Ce	88.8	89.6	GEA (¹⁴¹ Ce in whole A solution)
¹⁵³ Sm	84.2	83	ICP-OES (Stable Sm)
¹⁵⁶ Eu	93.1	85.8	GEA (¹⁵² Eu)
¹⁶¹ Tb	101	90.5	ICP-OES (Stable Tb)
U	57.2	90.4	KPA
²³⁹ Np	81.5	90.9	GEA (²³⁷ Np)

DU = depleted uranium; GEA = gamma energy analysis; HEU = highly enriched uranium; ICP-MS = inductively coupled plasma mass spectrometry; ICP-OES = inductively coupled plasma optical emission spectroscopy; KPA = kinetic phosphorescence analysis; RSD = relative standard deviation

6.0 Comparison of FY 2021 Results to Historical Campaigns and Literature Values

The results from the determination of R-values are included below in this section; the FY 2021 results are compared to previous irradiations in FY 2013, FY 2014, FY 2015, FY 2017, and FY 2018 where possible. The results are both plotted and tabulated, allowing for better comparisons of the historical data. The historical data include results that were not reported. These values are for comparison of techniques, previous reports should be examined for further detail on the reported data. Multiple data bases are used in this comparison, including the ENDF database from England and Rider (1994), the JEFF database from the JEFF Report 22 (Santamarina et al. 2009), and the JENDL database from Shibata et al. (2011).

6.1 Strontium-89

Historically, ^{89}Sr was analyzed by liquid scintillation counting (LSC), but recently the TIMS technique has improved to the point where it is being used as the primary method for the analysis of ^{89}Sr . The data from TIMS comes with the lowest uncertainty of any technique used in the radiochemical analysis of fission products. The results correlate very well among the years as well as with the literature R-value (see Figure 6.1 and Table 6.1).

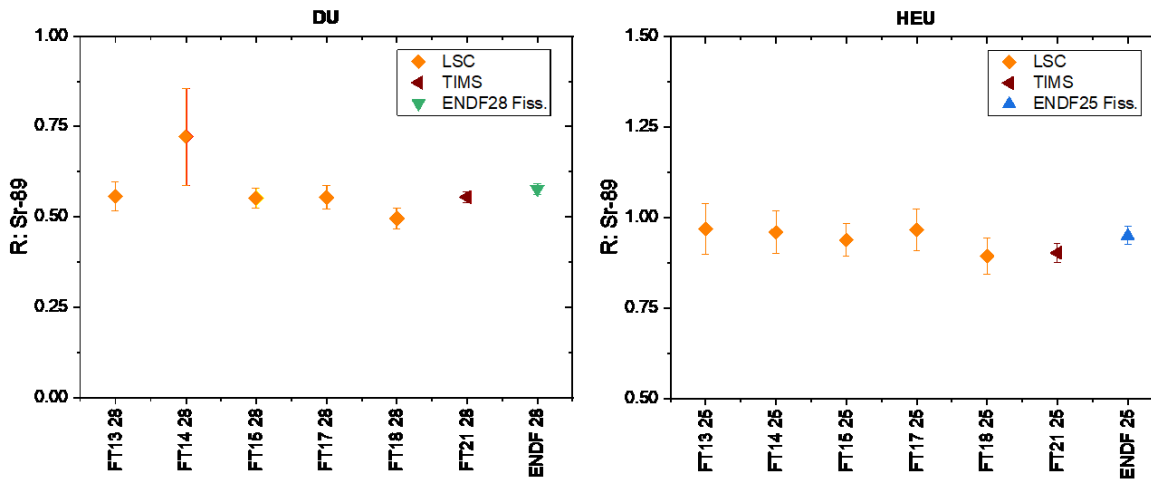


Figure 6.1. Strontium-89 R-values for DU and HEU samples irradiated on the Flattop critical assembly compared to previous R-value campaigns and ENDF ($R \pm 1\sigma$).

Table 6.1. Strontium-89 R-values for DU and HEU samples irradiated on the Flattop critical assembly compared to previous R-value campaigns and ENDF (R \pm 1 σ %).

	DU						
	FY 2013	FY 2014	FY 2015	FY 2017	FY 2018	FY 2021	ENDF
RC-TIMS	N/A	N/A	N/A	N/A	N/A	0.555 \pm 2.77%	0.578 \pm 2.62%
RC-LSC	0.557 \pm 7.22%	N/A	0.552 \pm 4.96%	0.554 \pm 6.04%	N/A	N/A	
RC-GEA	N/A	0.722 \pm 18.56%	0.611 \pm 7.66%	N/A	0.495 \pm 5.65%	N/A	
	HEU						
	FY 2013	FY 2014	FY 2015	FY 2017	FY 2018	FY 2021	ENDF
RC-TIMS	N/A	N/A	N/A	N/A	N/A	0.902 \pm 2.87%	0.950 \pm 2.62%
RC-LSC	0.968 \pm 7.22%	0.959 \pm 6.02%	0.938 \pm 4.73%	0.966 \pm 6.04%	N/A	N/A	
RC-GEA	N/A	N/A	0.984 \pm 6.91%	N/A	0.893 \pm 5.54%	N/A	

DU = depleted uranium; ENDF = Evaluated Nuclear Data File; HEU = highly enriched uranium; N/A = not applicable; RC-GEA = rad chem gamma energy analysis; RC-LSC = rad chem liquid scintillation counting; RC-TIMS = rad chem thermal ionization mass spectrometry

6.2 Yttrium-91

Yttrium-91 is analyzed at multiple locations in the radiochemical analysis scheme; it is analyzed by GEA in the A solution, a separated fraction yielding by an inductively coupled plasma (ICP) technique, and in a Compton suppressed sample. The measured R-value results are shown in Figure 6.2 and Table 6.2. As noted above in Section 3.2.2, a potential chemical yielding issue was found in yttrium analysis by ICP-OES or ICP-MS. An alternative separation method was used for the lanthanide fission product separation, with the aim of drastically decreasing overall separation time. As a consequence of using this procedure, the mass stable yttrium tracer added was decreased significantly, revealing a source of yttrium that was otherwise unaccounted for in previous efforts due to the higher yttrium concentrations. Historical correlation is excellent with low uncertainty, which could be used to produce an improvement of the literature value.

An absolute fission yield can be calculated using Eq.3 to provide an improved value for the thermal fission yield, a similar treatment will be applied to ^{136}Cs . Where the atoms/g are the atoms detected of ^{91}Y per gram of the A solution, and fission/g are the number of fissions per gram in the A solution. An example of both the absolute and relative cumulative fission yields are included in Appendix A.2

$$CFY = \frac{\text{Atoms/g}}{\text{Fissions/g}} \quad \text{Eq.3}$$

A comparison can be made between a fission yield obtained from the absolute fission yields and the relative CFY calculated through the rearrangement of **Error! Reference source not found.** using the CFY for a given isotope rather than the detected number of atoms. It should be noted that the absolute fission yield is detector specific, great effort is taken to ensure that all detectors are calibrated to the same sources to minimize or correct these potential differences. In the case of ^{91}Y counts obtained from the A solution, there are no detector differences, while there are some differences in a separated fraction.

The calculated absolute fission yield was calculated using [Error! Reference source not found.](#) using data obtained from Seiner et al. (2020) , as an average of the multiple replicates from data analyzed from GEA by multiple separation methods. A value of $0.0521 \pm 6.8\%$ was calculated. Using this value in [Error! Reference source not found.](#), a relative CFY can be calculated for both DU and HEU. Both relative and absolute fission yields are included in Table 6.3. The values for DU have significant uncertainties due to the uncertainty associated with the A solution analysis, but are within reason to the ENDF value. The values obtained for the HEU also have a significant uncertainty, but are well below that presented in the ENDF value (e.g., 12.5% compared to 64%). The relative CFY is significantly lower than the ENDF value as well as the absolute value. This is due to the low R-value obtained from the FY 2021 analysis. The lack of agreement highlights the need to continue these measurements to make sure better nuclear data can be produced for all isotopes.

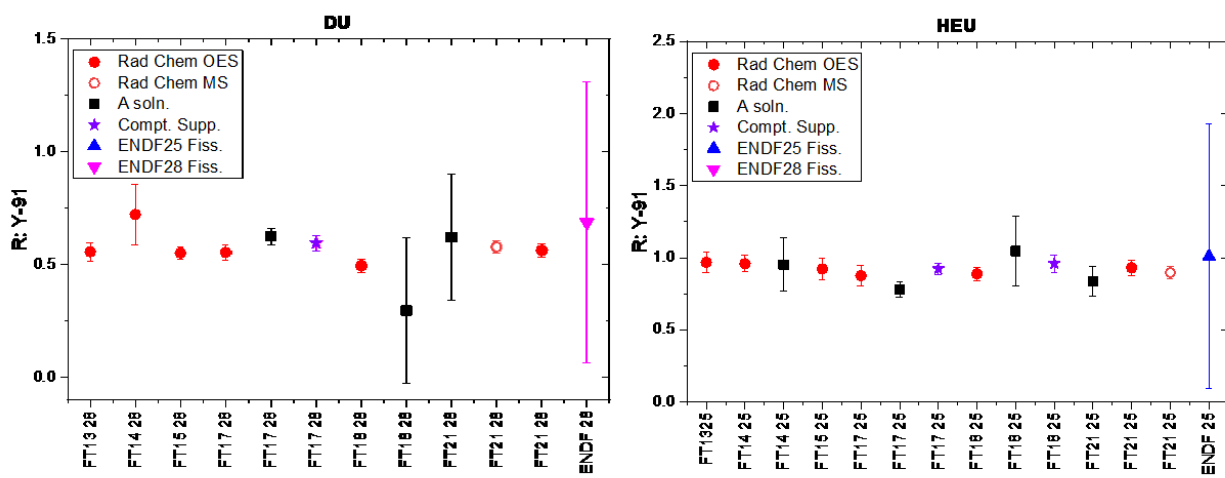


Figure 6.2. Yttrium-91 R-values for DU sample irradiated on the Flattop critical assembly compared to previous R-value campaigns and ENDF ($R \pm 1\sigma$). The R-Values for HEU and DU are separated by a dashed line and are labeled as either HEU or DU. Propagation of uncertainty does not include the high uncertainty in the CFY for yttrium-91.

Table 6.2. Yttrium-91 R-values for DU and HEU samples irradiated on the Flattop critical assembly compared to previous R-value campaigns and ENDF ($R \pm 1\sigma\%$). Propagation of uncertainty does not include the high uncertainty in the CFY for yttrium-91.

DU							
	FY 2013	FY 2014	FY 2015	FY 2017	FY 2018	FY 2021	ENDF
A Solution*	N/A	7.19 \pm 2.00%	5.97 \pm 8.57%	0.63 \pm 5.79%	0.611 \pm 2.95%	0.621 \pm 44.9%*	0.686 \pm 90.5%
RC-OES	N/A	N/A	N/A	0.622 \pm 7.40%	0.581 \pm 6.12%	0.563 \pm 5.53%	
RC-MS	N/A	N/A	N/A	N/A	N/A	0.578 \pm 4.46%	
Compton Suppression	N/A	N/A	N/A	0.60 \pm 5.77%	N/A	N/A	
HEU							
	FY 2013	FY 2014	FY 2015	FY 2017	FY 2018	FY 2021	ENDF
A Solution*	N/A	0.95 \pm 19.25%	0.95 \pm 19.25%	0.78 \pm 6.75%	0.931 \pm 4.25%	0.839 \pm 12.4%*	1.01 \pm 90.5%
RC-OES	N/A	N/A	N/A	0.876 \pm 8.07%	0.893 \pm 5.54%	0.931 \pm 5.83%	
RC-MS	N/A	N/A	N/A	N/A	N/A	0.897 \pm 4.25%	
Compton Suppression	N/A	N/A	N/A	0.92 \pm 4.46%	0.964 \pm 6.25%	N/A	
A Solution*	N/A	0.95 \pm 19.25%	0.95 \pm 19.25%	0.78 \pm 6.75%	0.931 \pm 4.25%	0.839 \pm 12.4%*	

*Due to contamination of stable Y, only the A solution value should be considered reliable.
DU = depleted uranium; ENDF = Evaluated Nuclear Data File; HEU = highly enriched uranium; N/A = not applicable; RC-MS = rad chem mass spectrometry; RC-OES = rad chem optical emission spectroscopy

Table 6.3. Relative and Absolute CFY for ^{91}Y . Values were obtained only for FY 2021 data, uncertainties are the propagated from the individual uncertainties. A solution values are used, due to the contamination of stable Y in the OES and MS samples.

	FY 2021 A solution Relative	FY 2021 A solution Absolute	ENDF
DU	0.0327 \pm 46%	0.0379 \pm 45%	0.0404 \pm 64%
HEU	0.0425 \pm 14.2%	0.0513 \pm 12.4%	0.0573 \pm 64%

DU = depleted uranium; ENDF = Evaluated Nuclear Data File; HEU = highly enriched uranium

6.3 Zirconium-95

Zirconium-95 is analyzed by GEA in the A solution. The results of the Flattop campaigns are shown in Figure 6.3 and Table 6.4. Historical correlation is excellent, providing data that agree with the literature value with similar uncertainty.

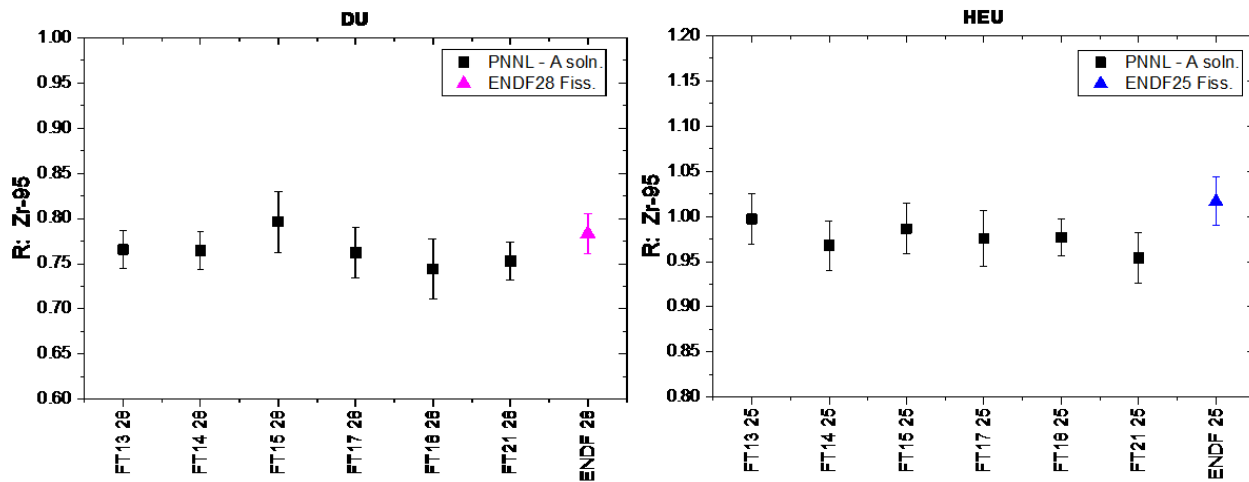


Figure 6.3. Zirconium-95 R-values for DU and HEU samples irradiated on the Flattop critical assembly compared to previous R-value campaigns and ENDF ($R \pm 1\sigma$).

Table 6.4. Zirconium-95 R-values for DU and HEU samples irradiated on the Flattop critical assembly compared to previous R-value campaigns and ENDF ($R \pm 1\sigma\%$).

DU							
	FY 2013	FY 2014	FY 2015	FY 2017	FY 2018	FY 2021	ENDF
A Solution	$0.77 \pm 2.80\%$	$0.76 \pm 2.67\%$	$0.796 \pm 4.26\%$	$0.76 \pm 3.61\%$	$0.752 \pm 4.24\%$	$0.753 \pm 2.83\%$	$0.783 \pm 2.80\%$
HEU							
	FY 2013	FY 2014	FY 2015	FY 2017	FY 2018	FY 2021	ENDF
A Solution	$1.00 \pm 2.79\%$	$0.97 \pm 2.83\%$	$0.986 \pm 2.83\%$	$0.98 \pm 3.13\%$	$0.982 \pm 2.66\%$	$0.954 \pm 2.91\%$	$1.02 \pm 2.62\%$

DU = depleted uranium; ENDF = Evaluated Nuclear Data File; HEU = highly enriched uranium

6.4 Zirconium-97

Zirconium-97 is analyzed by GEA in the A solution. The results of the Flattop campaigns are shown in Figure 6.4 and Table 6.5. Historical correlation is excellent, providing data that agree with the literature value with similar uncertainty.

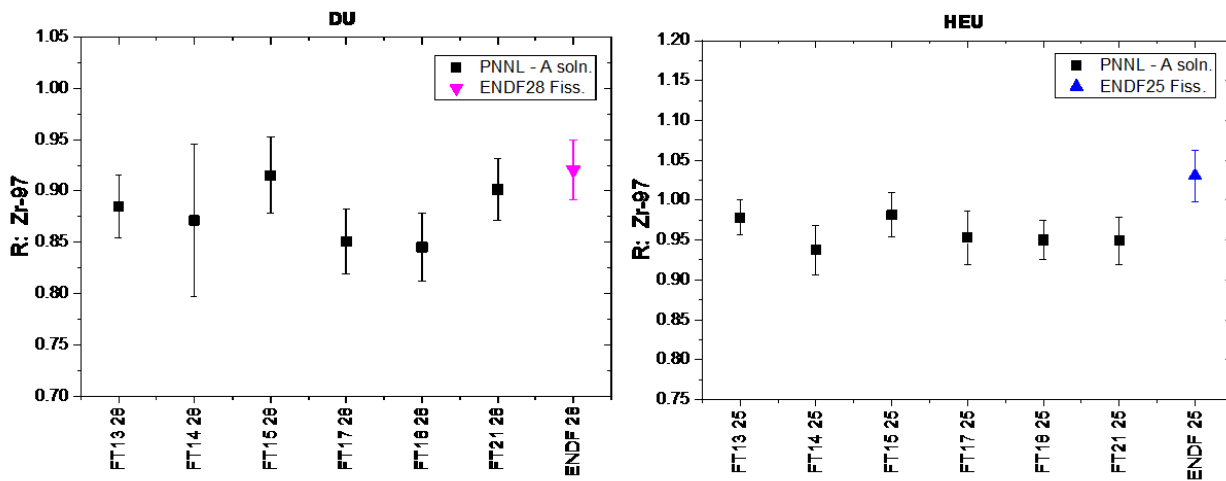


Figure 6.4. Zirconium-97 R-values for DU and HEU samples irradiated on the Flattop critical assembly compared to previous R-value campaigns and ENDF ($R \pm 1\sigma$).

Table 6.5. Zirconium-97 R-values for DU and HEU samples irradiated on the Flattop critical assembly compared to previous R-value campaigns and ENDF ($R \pm 1\sigma\%$).

DU							
	FY 2013	FY 2014	FY 2015	FY 2017	FY 2018	FY 2021	ENDF
A Solution	$0.89 \pm 3.50\%$	$0.87 \pm 8.51\%$	$0.915 \pm 4.05\%$	$0.85 \pm 3.70\%$	$0.845 \pm 4.28\%$	$0.901 \pm 3.33\%$	$0.921 \pm 3.14\%$
HEU							
	FY 2013	FY 2014	FY 2015	FY 2017	FY 2018	FY 2021	ENDF
A Solution	$0.98 \pm 2.24\%$	$0.94 \pm 3.30\%$	$0.982 \pm 2.87\%$	$0.95 \pm 3.52\%$	$0.954 \pm 3.05\%$	$0.949 \pm 3.13\%$	$1.03 \pm 3.14\%$

DU = depleted uranium; ENDF = Evaluated Nuclear Data File; HEU = highly enriched uranium

6.5 Ruthenium-103

Ruthenium-103 is analyzed by GEA in the A solution, the results from PNNL campaigns are shown in Figure 6.5 and Table 6.6. There is excellent agreement between the campaigns for DU targets, though the R-values produced are noticeably lower than the literature value but are within reason, compared to each other. This may be an indication that the methods employed by PNNL to determine this value or the nuclear data may need refinement. This is not the case for the HEU samples, where there is some variation between campaigns, but the average of the campaigns appears to match the literature value.

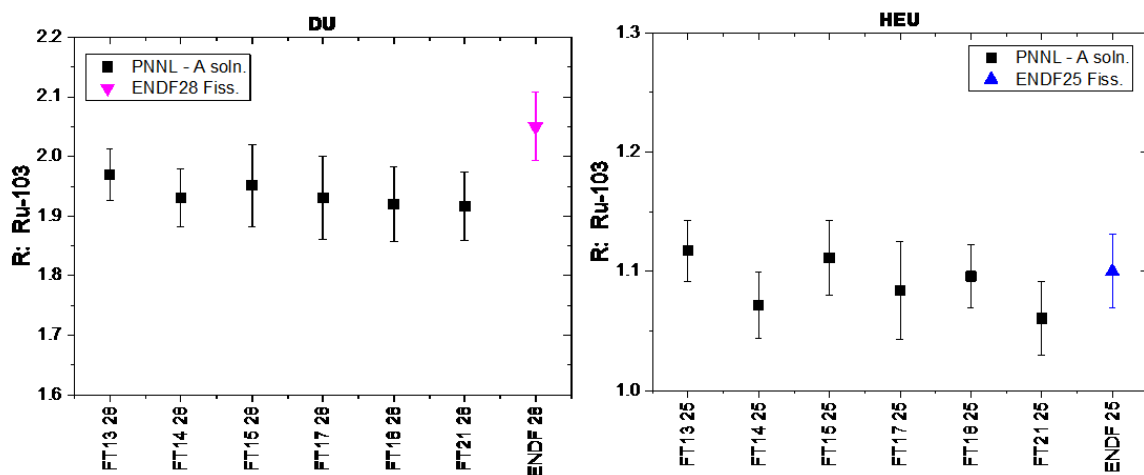


Figure 6.5. Ruthenium-103 R-values for DU and HEU samples irradiated on the Flattop critical assembly compared to previous R-value campaigns and ENDF ($R \pm 1\sigma$).

Table 6.6. Ruthenium-103 R-values for DU and HEU samples irradiated on the Flattop critical assembly compared to previous R-value campaigns and ENDF ($R \pm 1\sigma\%$).

DU							
	FY 2013	FY 2014	FY 2015	FY 2017	FY 2018	FY 2021	ENDF
A Solution	1.97 ± 2.18%	1.93 ± 2.55%	1.95 ± 3.53%	1.93 ± 3.61%	1.93 ± 3.46%	1.92 ± 3.02%	2.05 ± 2.80%
HEU							
	FY 2013	FY 2014	FY 2015	FY 2017	FY 2018	FY 2021	ENDF
A Solution	1.12 ± 2.27%	1.07 ± 2.59%	1.11 ± 2.79%	1.08 ± 3.77%	1.10 ± 2.83%	1.06 ± 2.91%	1.10 ± 2.80%

DU = depleted uranium; ENDF = Evaluated Nuclear Data File; HEU = highly enriched uranium

6.6 Silver-111

Silver-111 can be a challenge to detect and requires separation to analyze it properly. Results from all campaigns are shown in Figure 6.6 and Table 6.7. In previous campaigns, the A solution analysis was not included in the reporting due to spectral interferences, but it is of use for the comparison to the values obtained from the separated fractions. In the case of the FY 2021 DU (Z11050), ^{111}Ag was detectable but had significant amount uncertainty. The FY 2021 HEU (Z11051) A solution produced an R-value that was in excellent agreement with the separated fraction as well as with literature, though with higher uncertainties. When comparing the campaigns, one can see a variation in the results, particularly in FY 2015 where the R-value produced was significantly higher. The use of Compton suppression, while using the PNNL r_{his} value produced R-values that are higher than the literature value.

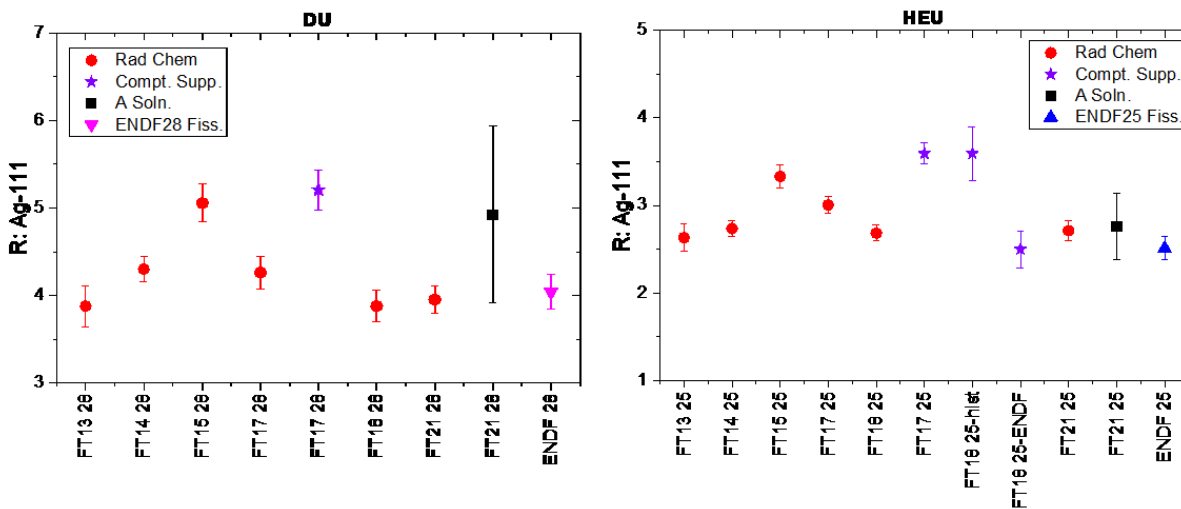


Figure 6.6. Silver-111 R-values for HEU and DU samples irradiated on Flattop critical assembly compared to previous R-value campaigns and ENDF ($R \pm 1\sigma$).

Table 6.7. Silver-111 R-values for DU and HEU samples irradiated on the Flattop critical assembly compared to previous R-value campaigns and ENDF ($R \pm 1\sigma\%$).

DU							
	FY 2013	FY 2014	FY 2015	FY 2017	FY 2018	FY 2021	ENDF
A Solution	N/A	N/A	N/A	N/A	N/A	$4.93 \pm 20.5\%$	$4.05 \pm 4.89\%$
RC-GEA	$3.88 \pm 6.07\%$	$4.30 \pm 3.30\%$	$5.056 \pm 4.29\%$	$4.265 \pm 4.35\%$	$3.88 \pm 4.91\%$	$3.95 \pm 3.85\%$	
Compton. Suppression	N/A	N/A	N/A	$3.621 \pm 4.47\%$	N/A	N/A	
HEU							
	FY 2013	FY 2014	FY 2015	FY 2017	FY 2018	FY 2021	ENDF
A Solution	N/A	N/A	N/A	N/A	N/A	$2.76 \pm 13.95\%$	$2.51 \pm 5.27\%$
RC-GEA	$2.63 \pm 5.96\%$	$2.74 \pm 3.18\%$	$3.33 \pm 3.92\%$	$3.004 \pm 3.17\%$	$2.70 \pm 3.82\%$	$2.71 \pm 4.40\%$	
Compton. Suppression	N/A	N/A	N/A	$2.498 \pm 3.33\%$	$2.51 \pm 8.47\%$	N/A	

DU = depleted uranium; ENDF = Evaluated Nuclear Data File; HEU = highly enriched uranium; N/A = not applicable; RC-GEA = rad chem gamma energy analysis

6.7 Cadmium-115

Cadmium-115 is measured in a separated Cd fraction, or with the use of Compton suppression analysis of an A solution. Each analysis is the average of multiple individual counts, with the associated propagated uncertainty. The R-value results are shown in Figure 6.7 and Table 6.8. The A solution analysis is included for FY 2021, calculated the ENDF fission yields, but the value should be considered unreliable due to interferences and low fission yields. The results are highly consistent among the campaigns with some variation that effectively averages to the ENDF literature R-value. There appears to be a slight high bias relative to ENDF for both HEU and DU, it is possible that the r_{hist} requires refinement in more thermal calibration separations, more individual counts are necessary, or could be caused by an accounted-for variable or bias.

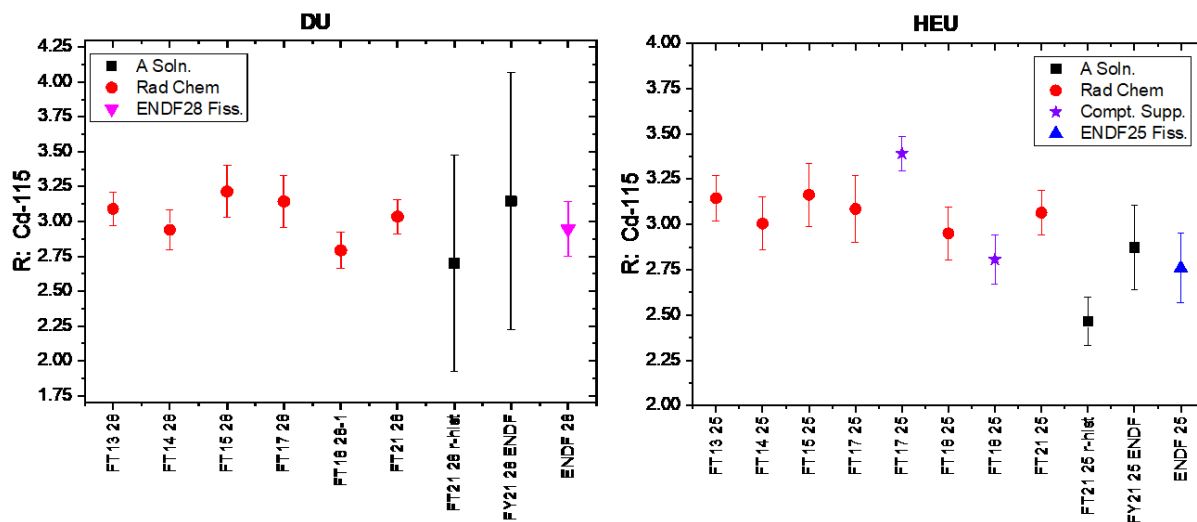


Figure 6.7. Cadmium-115 R-values for DU and HEU samples irradiated on the Flattop critical assembly compared to previous R-value campaigns and ENDF V.III.0 ($R \pm 1\sigma$).

Table 6.8. Cadmium-115 R-values for DU and HEU samples irradiated on the Flattop critical assembly compared to previous R-value campaigns and ENDF V.III.0 ($R \pm 1\sigma\%$).

DU							
	FY 2013	FY 2014	FY 2015	FY 2017	FY 2018	FY 2021	ENDF
A Solution	N/A	N/A	N/A	N/A	N/A	$2.70 \pm 28.7\%$	$2.95 \pm 6.63\%$
RC-GEA	$3.88 \pm 6.07\%$	$4.30 \pm 3.30\%$	$5.06 \pm 4.29\%$	$3.14 \pm 5.95\%$	$2.95 \pm 4.82\%$	$3.03 \pm 4.03\%$	
Compton. Suppression	N/A	N/A	N/A	N/A	N/A	N/A	
HEU							
	FY 2013	FY 2014	FY 2015	FY 2017	FY 2018	FY 2021	ENDF
A Solution	N/A	N/A	N/A	N/A	N/A	$2.46 \pm 5.40\%$	$2.76 \pm 6.91\%$
RC-GEA	$2.63 \pm 5.96\%$	$2.74 \pm 3.18\%$	$3.33 \pm 3.92\%$	$3.09 \pm 5.96\%$	$2.95 \pm 4.90\%$	$3.06 \pm 4.06\%$	
Compton. Suppression	N/A	N/A	N/A	$3.39 \pm 2.85\%$	$2.81 \pm 4.81\%$	N/A	

DU = depleted uranium; ENDF = Evaluated Nuclear Data File; HEU = highly enriched uranium; N/A = not applicable; RC-GEA = rad chem gamma energy analysis

6.8 Cadmium-115m

Cadmium-115m is measured in the separated Cd fraction by GEA, results are shown in Figure 6.8 and Table 6.9. The measurement requires the separation from other fission products due to the low branching ratios of ^{115m}Cd . These ratios are also coupled with high uncertainty, about 35%. Because of this, the uncertainty in the measurements is consequently high, typically greater than 30%. The R-value measured for DU over the multiple campaigns, had relatively large variability, while the HEU measured R-values were biased high relative to JEFF but were consistent. The high uncertainty in the gamma branching ratios and the inconsistencies in the results from the campaigns, particularly with DU, emphasize the need for further investigations into improving the individual isotope's uncertainty.

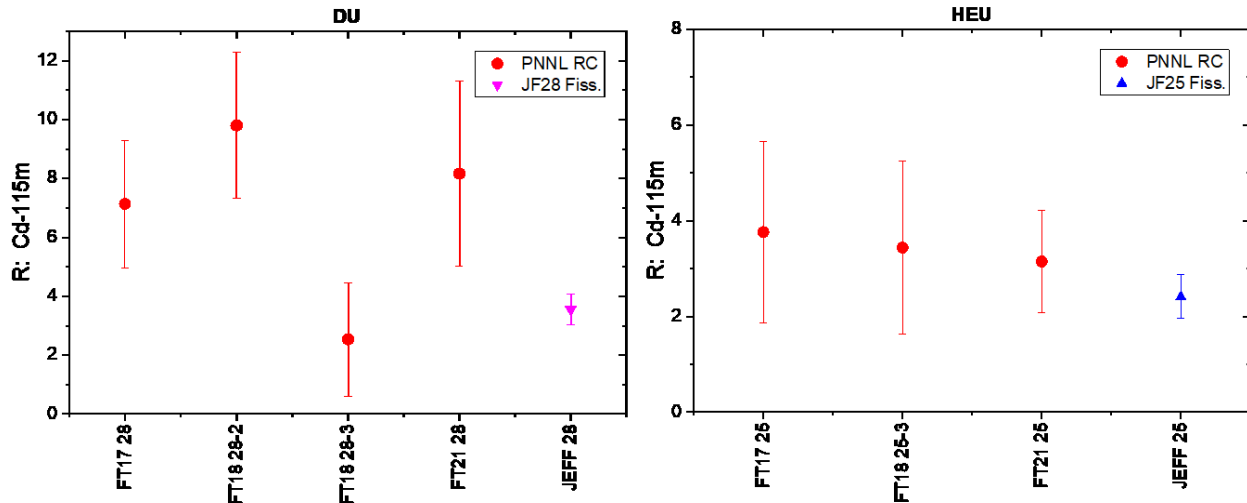


Figure 6.8. Cadmium-115m R-values for DU and HEU samples irradiated on the Flattop critical assembly compared to previous R-value campaigns and JEFF-3.1.1 ($R \pm 1\sigma$).

Table 6.9. Cadmium-115m R-values for DU and HEU samples irradiated on the Flattop critical assembly compared to previous R-value campaigns and JEFF3.1.1 ($R \pm 1\sigma\%$).

DU							
	FY 2013	FY 2014	FY 2015	FY 2017	FY 2018	FY 2021	JEFF 3.3
RC-GEA	N/A	N/A	N/A	7.14 30.30%	$2.54 \pm$ 75.90%	$8.17 \pm$ 38.5%	$3.07 \pm$ 8.71%
HEU							
	FY 2013	FY 2014	FY 2015	FY 2017	FY 2018	FY 2021	JEFF 3.3
RC-GEA	N/A	N/A	N/A	$3.77 \pm$ 50.20%	$3.45 \pm$ 52.61%	$3.15 \pm$ 33.9%	$2.86 \pm$ 23.85%

DU = depleted uranium; HEU = highly enriched uranium; JEFF = Joint Evaluated File for Fission and Fusion; N/A = not applicable; RC-GEA = rad chem gamma energy analysis

6.9 Tellurium-132

Tellurium-132 is a measured only in the A-solution GEA. Through all campaigns with either DU or HEU, all measured R-values are within reason to the ENDF literature R-value. Some variability in the R-value exists through the campaigns, with the DU being biased low, the FY 2013, FY 2014, and FY 2015 HEU R-values biased slightly high and the FY 2017, FY 2018, and FY 2021 R-values being biased low relative to the ENDF value (see Figure 6.9 and Table 6.10).

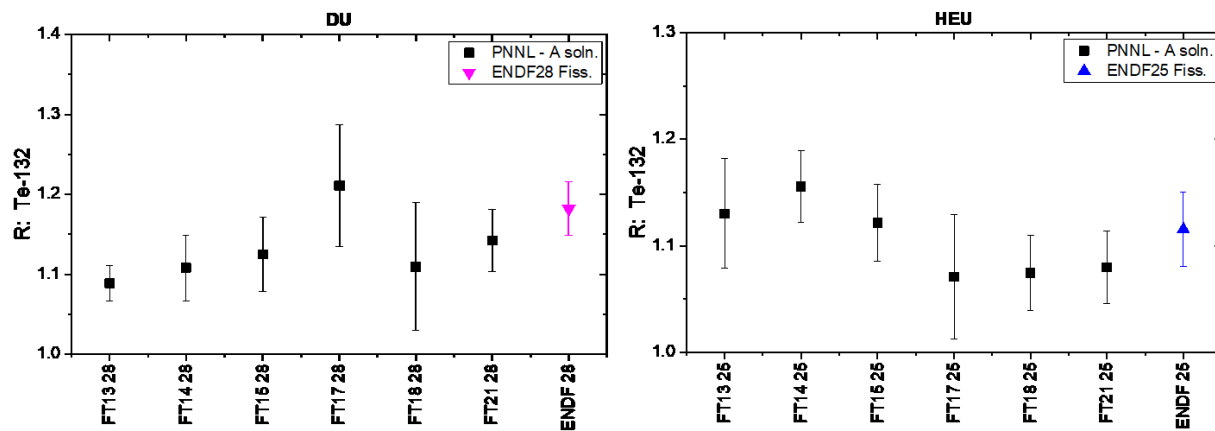


Figure 6.9. Tellurium-132 R-values for DU and HEU samples irradiated on the Flattop critical assembly compared to previous R-value campaigns and ENDF ($R \pm 1\sigma$).

Table 6.10. Tellurium-132 R-values for DU and HEU samples irradiated on the Flattop critical assembly compared to previous R-value campaigns and ENDF ($R \pm 1\sigma\%$).

DU							
	FY13	FY14	FY15	FY17	FY18	FY21	ENDF
A Solution	$1.09 \pm 2.04\%$	$1.11 \pm 3.70\%$	$1.13 \pm 4.16\%$	$1.21 \pm 6.26\%$	$1.14 \pm 6.58\%$	$1.14 \pm 3.40\%$	$1.18 \pm 2.80\%$
HEU							
	FY13	FY14	FY15	FY17	FY18	FY21	ENDF
A Solution	$1.13 \pm 4.56\%$	$1.16 \pm 2.89\%$	$1.12 \pm 3.21\%$	$1.07 \pm 5.43\%$	$1.08 \pm 4.94\%$	$1.08 \pm 3.13\%$	$1.12 \pm 3.14\%$

DU = depleted uranium; ENDF = Evaluated Nuclear Data File; HEU = highly enriched uranium

6.10 Cesium-136

Fission of ^{238}U with fission spectrum neutrons, ~ 2 MeV, does not produce significant quantities of ^{136}Cs due to the low fission yield of the fission product. This in turn produces a low R-value, and creates difficulty in the detection of ^{136}Cs . The uncertainty in the R-value is the result of the high uncertainty in the fission yields. Shown in the Figure 6.10 are the results of the R-value measurements from PNNL over the many Flattop campaigns for both DU and HEU targets. Similarly, the results are tabulated in Table 6.11. Note that a DU target was included in each of the campaigns including FY 2013, FY 2014, FY 2015, FY 2017, FY 2018, and FY 2021. Cesium-136 was only detected in FY 2013, FY 2018, and FY 2021. The R-values obtained from these measurements are lower than those included in ENDF but are highly consistent. This is an indication that it is likely possible to obtain better statistics on the fission yields for ^{136}Cs to reflect this lower uncertainty.

Conversely the R-value results obtained from HEU in all campaigns have been nearly identical to the ENDF value, though with significantly lower uncertainties. As was stated with the DU, the HEU ^{136}Cs fission yield uncertainty could be improved through the adoption of the PNNL data. Though included in the plot, the A solution analysis point in FY 2021 should be taken with a grain of salt, due to spectral interferences and will not be used in averages. However, it does demonstrate the feasibility of an A solution detection of ^{136}Cs . The average R-value obtained

from the many campaigns is $2.29 \pm 9.49\%$ (propagated uncertainty). Using data obtained from thermal irradiations could provide a large decrease in the fission yields used for this isotope.

A relative fission yield can be calculated using a revised ^{136}Cs yield obtained through a yearly thermal irradiation of ^{235}U performed at PNNL. An absolute cumulative thermal fission yield was calculated with data from Seiner et al. (2020). A value of $5.78 \times 10^{-5} \pm 7.57\%$ (0.00578%) was obtained using, the average from the two separate chemistries and their replicate data. This value can be compared to the ENDF V.III.0 value of $5.53 \times 10^{-5} \pm 64\%$, showing a clear improvement to the uncertainties.

This updated value incorporates a single thermal calibration campaign, however there are many more that could be included in the calculation, which should have a beneficial effect on the uncertainty. Rearrangement of **Error! Reference source not found.** allows for the calculation of the relative fission yield, incorporating the newly calculated thermal fission yield for ^{136}Cs and using the available literature fission yields. A value of $1.36 \times 10^{-4} \pm 17.8\%$ is obtained from this calculation, compared to the ENDF/B V.III.0 value of $1.17 \times 10^{-4} \pm 64\%$. An absolute fission yield can be calculated similarly to that obtained for the thermal fission, though for the FY 2021 R-value campaign. In this case a value of $1.28 \times 10^{-4} \pm 15.9\%$ is obtained, which is in good agreement with the relative fission yield value. Further refinement is required for these yield values, but this is a clear indication that the data obtained through these campaigns produce significant improvements to the fission yields.

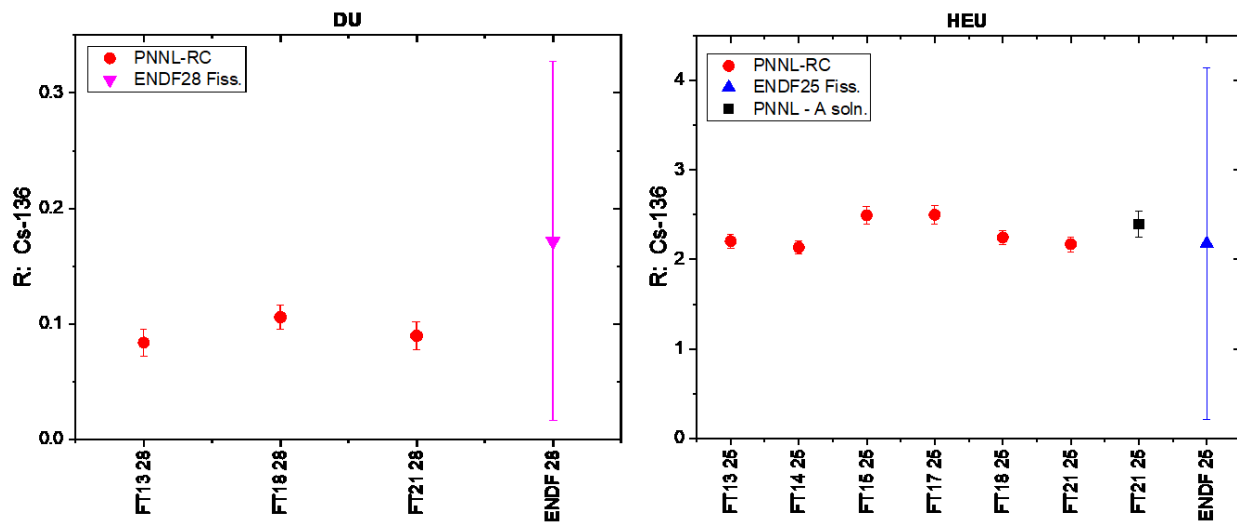


Figure 6.10. Left plot shows the Cs-136 R-values for DU sample, the right plot shows the HEU R-Values. Samples were irradiated on the Flattop critical assembly compared to previous R-value campaigns and ENDF ($R \pm 1\sigma$). Propagation of uncertainty does not include the high uncertainty in the CFY for ^{136}Cs .

Table 6.11. Cesium-136 R-values for DU and HEU samples irradiated on the Flattop critical assembly compared to previous R-value campaigns and ENDF ($R \pm 1\sigma\%$). Propagation of uncertainty does not include the high uncertainty in the CFY for ^{136}Cs .

DU							
	FY 2013	FY 2014	FY 2015	FY 2017	FY 2018	FY 2021	ENDF
RC-GEA	0.08 \pm 13.68%	N/A	N/A	N/A	0.106 \pm 2.95%	0.09 \pm 13.5%	0.172 \pm 90.5%
HEU							
	FY 2013	FY 2014	FY 2015	FY 2017	FY 2018	FY 2021	ENDF
A Solution	N/A	N/A	N/A	N/A	N/A	2.40 \pm 5.96%	2.18 \pm 90.5%
RC-GEA	2.20 \pm 3.43%	2.13 \pm 3.26%	2.49 \pm 4.11%	2.50 \pm 4.27%	2.26 \pm 3.96%	2.17 \pm 3.84%	

DU = depleted uranium; ENDF = Evaluated Nuclear Data File; HEU = highly enriched uranium; RC-GEA = rad chem gamma energy analysis

6.11 Cesium-137

Cesium-137 is analyzed in the A solution, as well as a separated fraction, and it can also be measured with the use of Compton suppression. Though it is not typically reported, the A solution ^{137}Cs is included as a comparison in the HEU plot, this value should be viewed as a lower-quality result due to spectral interferences. The R-values measured in all Flattop irradiation campaigns are shown in Figure 6.11 and Table 6.12. The measured R-values are consistent between the Flattop campaigns with some variation. Improvement to the separation and analysis is evident as the general trend in the results are narrowing in on the ENDF literature R-value. Separated fractions from radiochemistry, as well as the A solution analysis are an average of multiple individual counts, with associated propagated uncertainty.

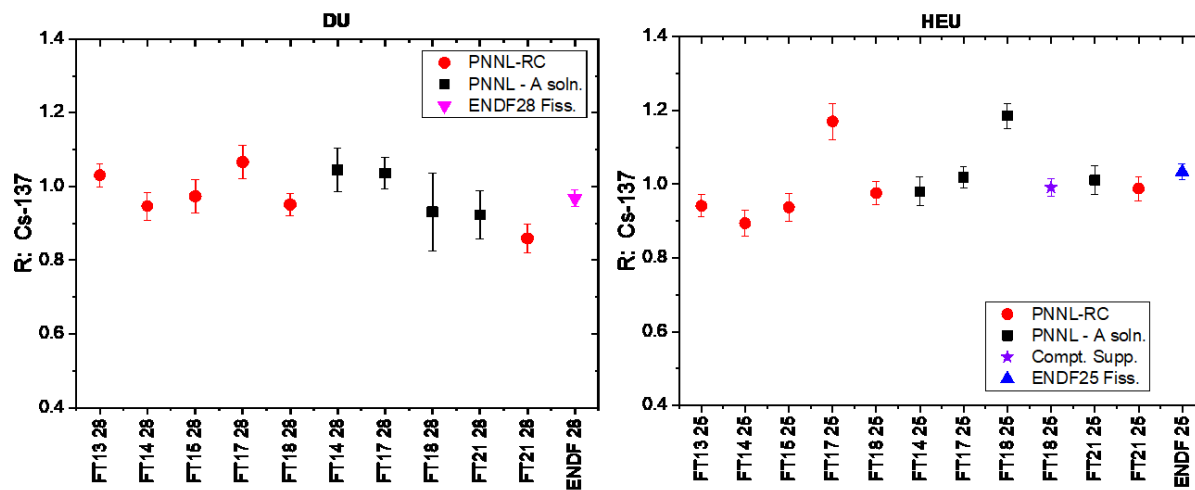


Figure 6.11. Cesium-137 R-values for DU and HEU samples irradiated on the Flattop critical assembly compared to previous R-value campaigns and ENDF ($R \pm 1\sigma\%$).

Table 6.12. Cesium-137 R-values for DU and HEU samples irradiated on the Flattop critical assembly compared to previous R-value campaigns and ENDF ($R \pm 1\sigma\%$).

DU

	FY 2013	FY 2014	FY 2015	FY 2017	FY 2018	FY 2021	ENDF
A Solution	N/A	1.04 ± 5.73%	N/A	1.04 ± 4.05%	1.02 ± 3.34%	0.923 ± 7.08%	0.969 ± 2.27%
RC-GEA	1.03 ± 3.04%	0.947 ± 3.98%	0.97 ± 4.59%	1.07 ± 4.18%	0.951 ± 3.63%	0.859 ± 4.62%	
Compton. Suppression	N/A	N/A	N/A	N/A	N/A	N/A	
HEU							
	FY 2013	FY 2014	FY 2015	FY 2017	FY 2018	FY 2021	ENDF
A Solution	N/A	0.98 ± 4.03%	N/A	1.02 ± 2.75%	1.06 ± 2.95%	1.01 ± 3.89%	1.03 ± 2.10%
RC-GEA	0.94 ± 3.16%	0.894 ± 4.04%	0.94 ± 4.07%	1.17 ± 4.15%	0.980 ± 3.83%	0.988 ± 3.34%	
Compton. Suppression	N/A				0.995 ± 2.39%	N/A	
DU = depleted uranium; ENDF = Evaluated Nuclear Data File; HEU = highly enriched uranium; RC-GEA = rad chem gamma energy analysis							

6.12 Barium-140

Barium-140 is measured in the A solution. There are few interferences, which allow for a simple analysis. R-value results from all Flattop campaigns are shown in Figure 6.12 and Table 6.13. The results are consistent among campaigns and compare within reason to the ENDF literature value. The HEU results are slightly low relative to the ENDF literature value.

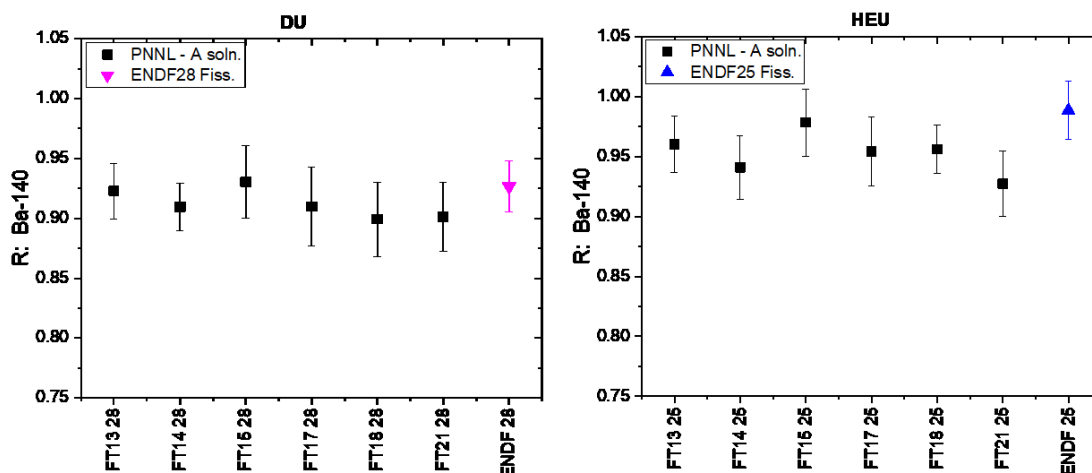


Figure 6.12. Barium-140 R-values for DU and HEU samples irradiated on the Flattop critical assembly compared to previous R-value campaigns and ENDF ($R \pm 1\sigma$).

Table 6.13. Barium-140 R-values for DU and HEU samples irradiated on the Flattop critical assembly compared to previous R-value campaigns and ENDF ($R \pm 1\sigma\%$).

DU							
	FY 2013	FY 2014	FY 2015	FY 2017	FY 2018	FY 2021	ENDF
A Solution	0.92 ± 2.51%	0.91 ± 2.19%	0.930 ± 3.26%	0.91 ± 3.61%	0.904 ± 3.49%	0.901 ± 3.32%	0.927 ± 2.33%
HEU							
	FY 2013	FY 2014	FY 2015	FY 2017	FY 2018	FY 2021	ENDF
A Solution	0.96 ± 2.44%	0.94 ± 2.80%	0.978 ± 2.86%	0.95 ± 3.04%	0.960 ± 2.78%	0.927 ± 2.91%	0.989 ± 2.43%

DU = depleted uranium; ENDF = Evaluated Nuclear Data File; HEU = highly enriched uranium

6.13 Cerium-141

Analysis of ^{141}Ce was conducted by GEA of the A solution. It is also used as an internal tracer for the other Ce isotopes in the separated Ce fractions. The results of the Flattop campaigns are shown in Figure 6.14 and Table 6.14. The measured R-values are consistent among campaigns and are within in reason to the ENDF literature value, though there is a slight low bias between the measured HEU and DU R-values relative to the ENDF value. The measured R-values are within 2σ to the ENDF value for both HEU and DU targets.

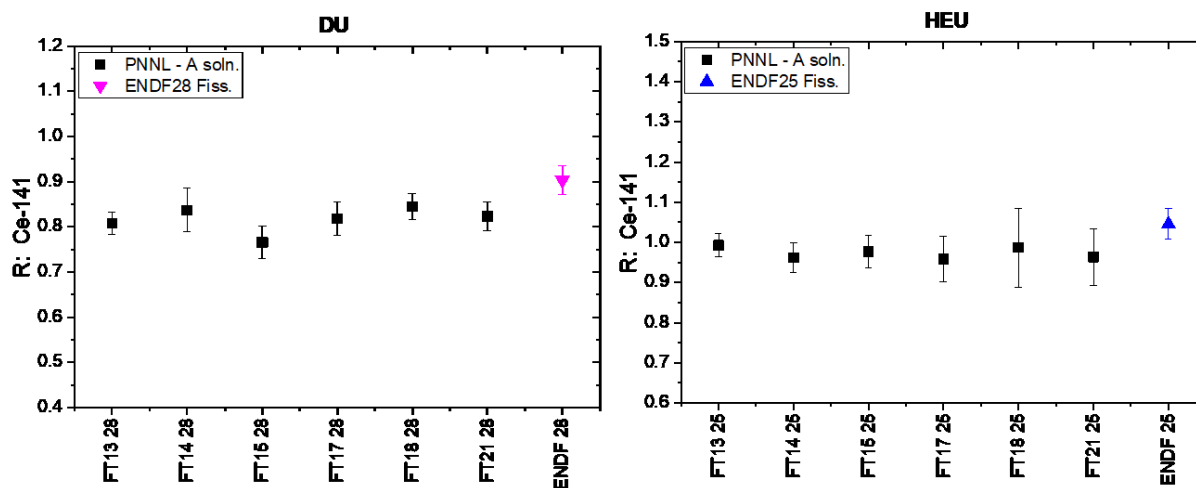


Figure 6.13. Cerium-141 R-values for DU and HEU samples irradiated on the Flattop critical assembly compared to previous R-value campaigns and ENDF ($R \pm 1\sigma\%$).

Table 6.14. Cerium-141 R-values for DU and HEU samples irradiated on the Flattop critical assembly compared to previous R-value campaigns and ENDF (R \pm 1 σ %).

DU							
	FY 2013	FY 2014	FY 2015	FY 2017	FY 2018	FY 2021	ENDF
A Solution	0.81 \pm 2.94%	0.84 \pm 5.80%	0.766 \pm 4.67%	0.82 \pm 4.51%	0.851 \pm 3.23%	0.823 \pm 3.94%	0.904 \pm 3.57%
HEU							
	FY 2013	FY 2014	FY 2015	FY 2017	FY 2018	FY 2021	ENDF
A Solution	0.99 \pm 2.94%	0.96 \pm 3.77%	0.977 \pm 4.05%	0.96 \pm 5.88%	1.00 \pm 6.24%	0.963 \pm 6.98%	1.05 \pm 3.57%

DU = depleted uranium; ENDF = Evaluated Nuclear Data File; HEU = highly enriched uranium

6.14 Cerium-143

Cerium-143 is measured by GEA of the A solution and as the separated fraction as an internal tracer. Results from all Flattop campaigns are shown in Figure 6.14 and Table 6.15. R-values through the campaigns for DU targets are highly consistent with little variation and are nearly identical to the ENDF R-value. However, there is a slight low bias for the HEU targets, with the bulk of the R-values being within 2 σ of the ENDF value.

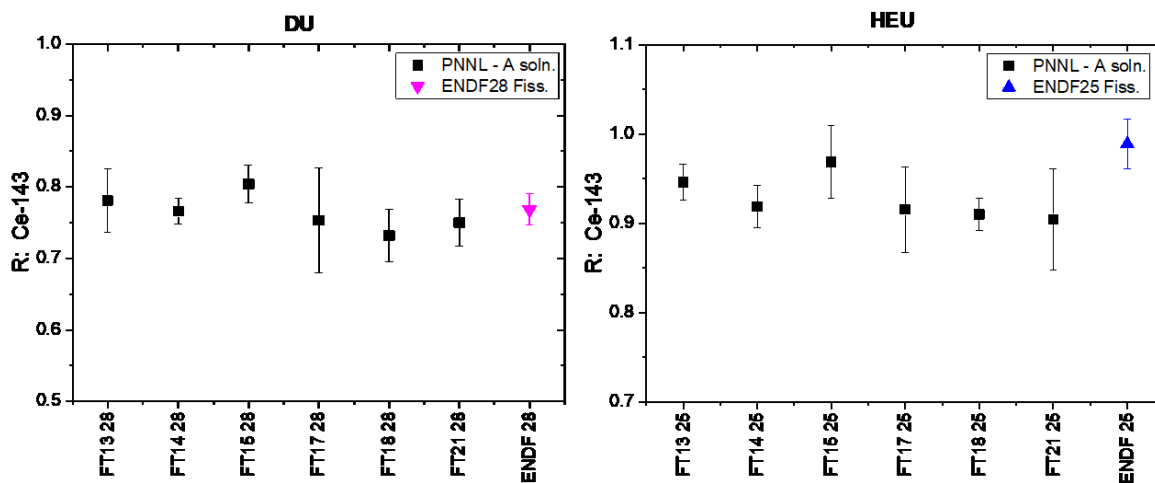


Figure 6.14. Cerium-143 R-values for DU and HEU samples irradiated on the Flattop critical assembly compared to previous R-value campaigns and ENDF (R \pm 1 σ).

Table 6.15. Cerium-143 R-values for DU and HEU samples irradiated on the Flattop critical assembly compared to previous R-value campaigns and ENDF (R $\pm 1\sigma\%$).

DU							
	FY 2013	FY 2014	FY 2015	FY 2017	FY 2018	FY 2021	ENDF
A Solution	0.78 \pm 5.67%	0.77 \pm 2.31%	0.804 \pm 3.26%	0.75 \pm 9.77%	0.732 \pm 5.22%	0.750 \pm 4.37%	0.769 \pm 2.80%
HEU							
	FY 2013	FY 2014	FY 2015	FY 2017	FY 2018	FY 2021	ENDF
A Solution	0.95 \pm 2.08%	0.92 \pm 2.54%	0.969 \pm 4.17%	0.92 \pm 5.25%	0.914 \pm 2.58%	0.904 \pm 6.23%	0.989 \pm 2.80%

DU = depleted uranium; ENDF = Evaluated Nuclear Data File; HEU = highly enriched uranium

6.15 Cerium-144

Analysis of ^{144}Ce is conducted by GEA of both the A solution and as a separated Ce fraction. Results from all Flattop campaigns are shown in Figure 6.15 and Table 6.16. The averages of the analysis of the analysis of the A solution or the separated fractions have been calculated: the A solution only averages are $0.866 \pm 23\%$ and $0.942 \pm 26\%$ and the separated fractions are $0.761 \pm 32\%$ and $0.923 \pm 17\%$ for DU and HEU respectively. There is a general trend in the separated fraction analysis, where the measured R-value is approaching the ENDF R-value, most specifically the DU targets. The overall average of both the A solution and separated fractions are $0.813 \pm 39\%$ and $0.932 \pm 31\%$ for DU and HEU respectively. The overall average of the DU R-values is nearly identical to the ENDF value, the HEU R-value is slightly lower than the ENDF value but is within 1σ .

The separation of Ce reflected the changes suggested in Degnan et al. (2019), but there was an issue in the separation—likely because of the age of the oxidant (sodium bromate). As a consequence of this issue, only a small fraction of the Ce was in the separated fraction. The remaining Ce was found in another fraction and analyzed with recovery of more than 88% for both DU and HEU.

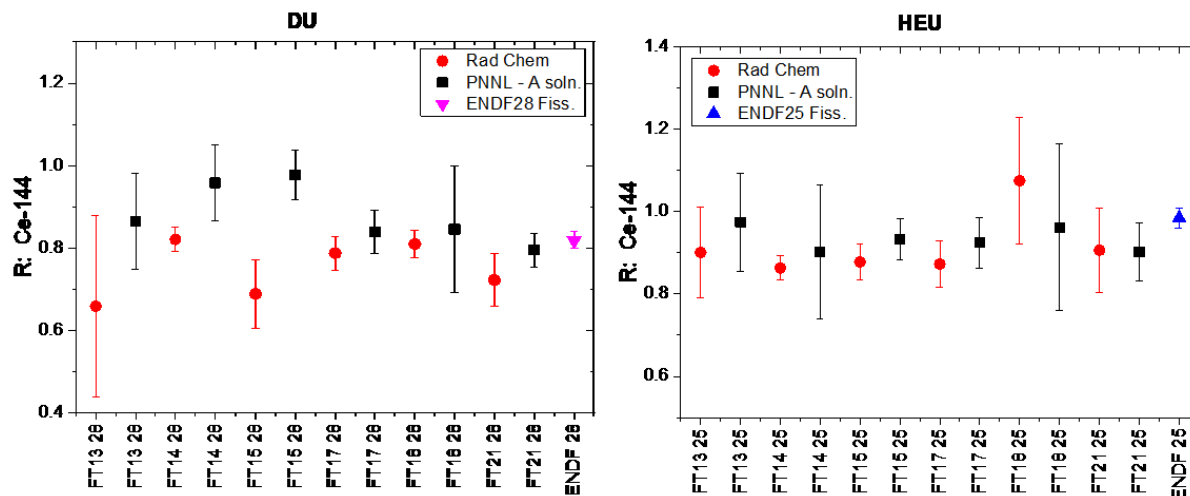


Figure 6.15. Cerium-144 R-values for DU and HEU samples irradiated on the Flattop critical assembly compared to previous R-value campaigns and ENDF (R $\pm 1\sigma\%$).

Table 6.16. Cerium-144 R-values for DU and HEU samples irradiated on the Flattop critical assembly compared to previous R-value campaigns and ENDF ($R \pm 1\sigma\%$).

DU							
	FY 2013	FY 2014	FY 2015	FY 2017	FY 2018	FY 2021	ENDF
A Solution	0.86 \pm 13.44%	0.96 \pm 9.55%	0.977 \pm 6.11%	0.84 \pm 6.25%	0.835 \pm 10.50%	0.722 \pm 8.72%	0.819 \pm 2.52%
RC-GEA	0.658 \pm 33.51%	0.821 \pm 3.61%	0.689 \pm 12.17%	0.788 \pm 5.18%	0.815 \pm 4.07%	0.795 \pm 5.15%	
HEU							
	FY 2013	FY 2014	FY 2015	FY 2017	FY 2018	FY 2021	ENDF
A Solution	0.97 \pm 12.25%	0.90 \pm 18.01%	0.933 \pm 5.43%	0.92 \pm 6.71%	1.02 \pm 2.80%	0.906 \pm 11.4%	0.985 \pm 2.52%
RC-GEA	0.901 \pm 12.18%	0.863 \pm 3.46%	0.878 \pm 4.91%	0.873 \pm 6.53%	1.12 \pm 3.91%	0.902 \pm 7.72%	

DU = depleted uranium; ENDF = Evaluated Nuclear Data File; HEU = highly enriched uranium; RC-GEA = rad chem gamma energy analysis

6.16 Neodymium-147

Neodymium-147 is analyzed by GEA of the A solution. The R-value results from all campaigns are shown in Figure 6.16 and Table 6.17. Consistency between campaigns is high, where all R-values are within 1σ between each individual campaign as well as the ENDF value.

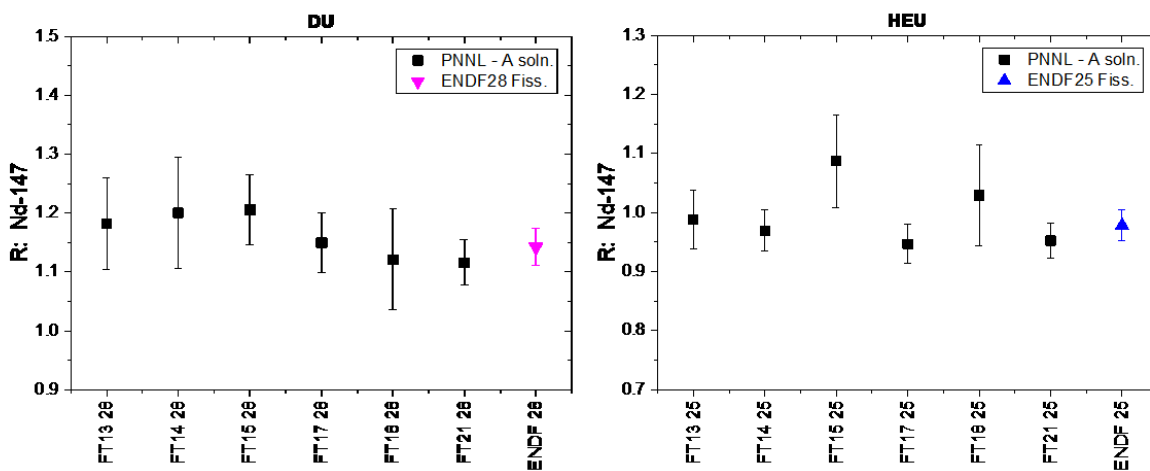


Figure 6.16. Neodymium-147 R-values for DU and HEU samples irradiated on the Flattop critical assembly compared to previous R-value campaigns and ENDF ($R \pm 1\sigma\%$).

Table 6.17. Neodymium-147 R-values for DU sample irradiated on the Flattop critical assembly compared to previous R-value campaigns and ENDF (R $\pm 1\sigma\%$).

DU							
	FY 2013	FY 2014	FY 2015	FY 2017	FY 2018	FY 2021	ENDF
A Solution	1.18 \pm 6.57%	1.20 \pm 7.86%	1.21 \pm 4.95%	1.15 \pm 4.43%	1.14 \pm 7.00%	1.16 \pm 3.48%	1.14 \pm 2.80%
HEU							
	FY 2013	FY 2014	FY 2015	FY 2017	FY 2018	FY 2021	ENDF
A Solution	0.99 \pm 5.05%	0.97 \pm 3.60%	3.26 \pm 2.62%	0.95 \pm 3.52%	1.04 \pm 3.50%	0.952 \pm 3.07%	0.979 \pm 2.62%

DU = depleted uranium; ENDF = Evaluated Nuclear Data File; HEU = highly enriched uranium

6.17 Samarium-153

Samarium-153 analysis was conducted by GEA of the separated fractions at PNNL with yielding by ICP-OES. The results for DU and HEU from each of the Flattop campaigns are shown in Figure 6.17 and Table 6.18. An interlaboratory calibration and comparison study for ^{153}Sm , Jackson et. al. (2018) discovered that ^{153}Sm thermal ^{235}U CFY reported in ENDF/B-VII.I (0.158%) is 15% higher than it should be and should be closer to 0.135%. The CFY reported by Jackson et. al. (2018) produced a $\text{CFY}_{\text{Sm-153}} / \text{CFY}_{\text{Mo-99}}$ ratio of 0.0221, which consequently raised the R-value reported. The calculated R-values from FY 2021 reflected these changes.

The DU R-values over the Flattop campaigns are not as consistent as the R-values measured from HEU, there is variability between campaigns, and they were about 14.4% lower than the ENDF value. Examining only the FY 2021 data (the data that reflect the suggested CFY), the R-value is still well below the ENDF R-value. The ENDF R-value considers the ^{238}U thermal yields of the ^{153}Sm , which could possibly use refinement.

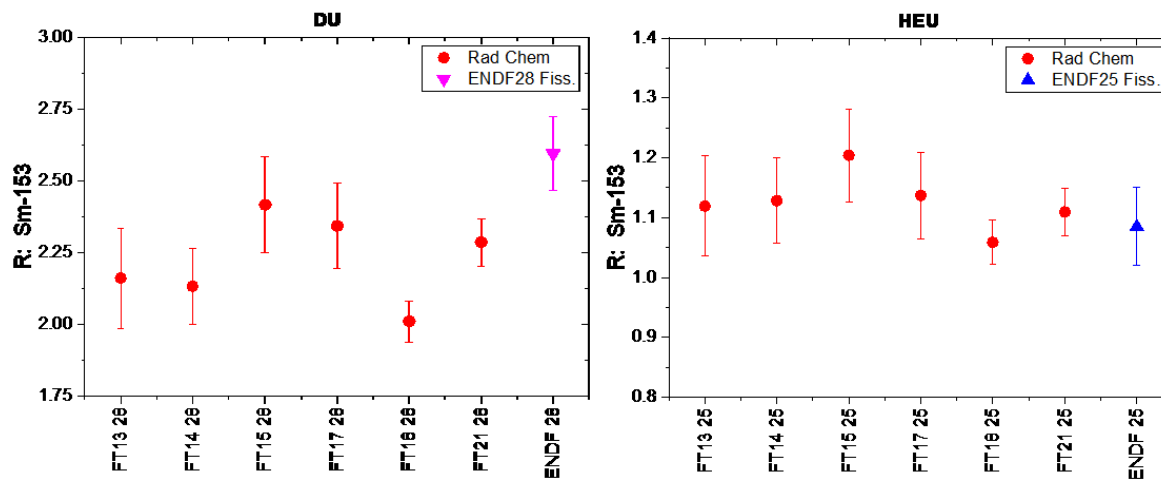


Figure 6.17. Samarium-153 R-values for DU sample irradiated on the Flattop critical assembly compared to previous R-value campaigns and ENDF (R $\pm 1\sigma\%$); open symbols denote R-Values calculated using the ^{153}Sm CFY reported in Jackson et al. 2018.

Table 6.18. Samarium-153 R-values for DU sample irradiated on the Flattop critical assembly compared to previous R-value campaigns and ENDF ($R \pm 1\sigma\%$)

DU							
	FY 2013	FY 2014	FY 2015	FY 2017	FY 2018	FY 2021	ENDF
RC-GEA	2.16 \pm 8.08%	2.13 \pm 6.24%	2.42 \pm 6.92%	2.34 \pm 6.33%	2.01 \pm 3.91%	2.29 \pm 3.62%	2.60 \pm 4.89%
HEU							
	FY 2013	FY 2014	FY 2015	FY 2017	FY 2018	FY 2021	ENDF
RC-GEA	1.12 \pm 7.46%	1.13 \pm 6.28%	1.20 \pm 6.42%	1.14 \pm 6.40%	1.06 \pm 3.90%	1.11 \pm 5.57%	1.27 \pm 6.47%

DU = depleted uranium; ENDF = Evaluated Nuclear Data File; HEU = highly enriched uranium; RC-GEA = rad chem gamma energy analysis

6.18 Europium-156

Europium-156 is analyzed done using GEA of a separated fraction, although the measurement can be made in the A solution by GEA (not typically reported). Yielding of the ^{156}Eu is done using two methods, ICP-OES of stable Eu carrier, as well as radiotracer ^{152}Eu analysis by GEA. Results from all R-value campaigns are shown in Figure 6.18 and Table 6.19. Both R-values obtained from each method were included for FY 2021, but only GEA was included for any other campaign. One of the obstacles of the analysis of ^{156}Eu is the potential for the fractionation of ^{156}Eu and ^{156}Sm at short times. In the case of the FY 2021 campaign, this was not an issue even when considering the shorter-than-usual separation times; there was more than sufficient time between the separation and the irradiation (irradiation began April 12; the sample was received April 20, and separation of Eu/Sm separation took place April 22).

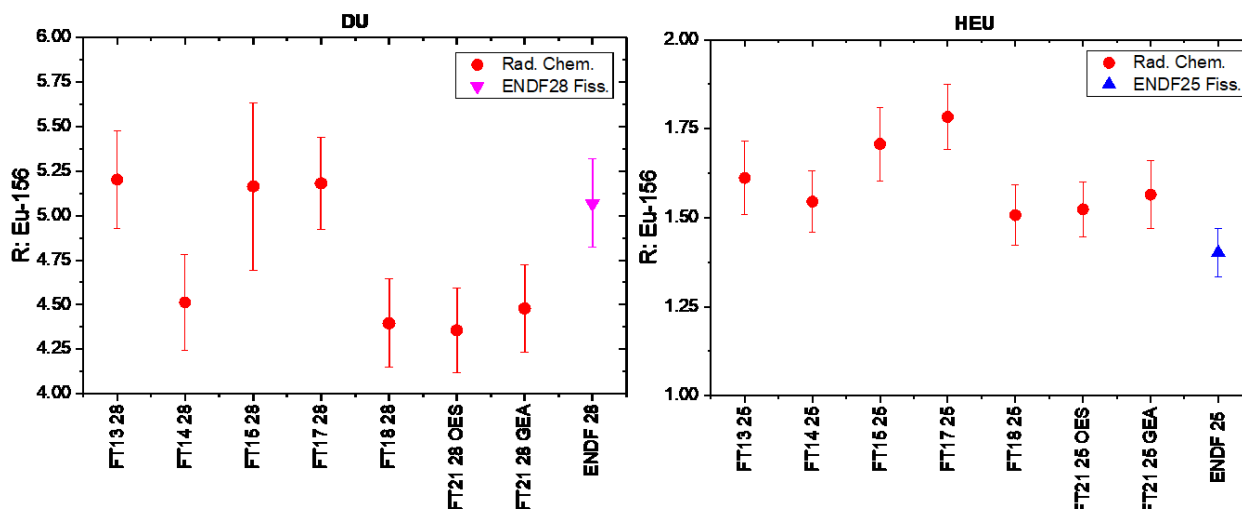


Figure 6.18. Europium-156 R-values for DU sample irradiated on the Flattop critical assembly compared to previous R-value campaigns and ENDF ($R \pm 1\sigma$).

Table 6.19. Europium-156 R-values for DU sample irradiated on the Flattop critical assembly compared to previous R-value campaigns and ENDF ($R \pm 1\sigma\%$).

DU							
	FY 2013	FY 2014	FY 2015	FY 2017	FY 2018	FY 2021	ENDF
A Solution	N/A	N/A	N/A	N/A	4.69 \pm 4.66%	4.08 \pm 12.5%	5.07 \pm 4.89%
RC-GEA	5.20 \pm 5.30%	4.51 \pm 5.96%	5.16 \pm 9.10%	5.18 \pm 5.03%	4.40 \pm 5.88%	4.48 \pm 5.46%	
RC-OES	N/A	N/A	N/A	N/A	N/A	4.36 \pm 5.46%	
HEU							
	FY 2013	FY 2014	FY 2015	FY 2017	FY 2018	FY 2021	ENDF
A Solution	N/A	N/A	N/A	N/A	1.67 \pm 51.57%	N/A	1.40 \pm 4.89%
RC-GEA	1.61 \pm 6.40%	1.55 \pm 5.61%	1.71 \pm 6.04%	1.78 \pm 5.12%	1.51 \pm 5.84%	1.57 \pm 6.04%	
RC-OES	N/A	N/A	N/A	N/A	N/A	1.52 \pm 5.11%	

DU = depleted uranium; ENDF = Evaluated Nuclear Data File; HEU = highly enriched uranium; RC-GEA = rad chem gamma energy analysis; RC-OES = rad chem optical emission spectroscopy

6.19 Terbium-161

Analysis of ^{161}Tb presents a unique challenge, requiring separation from other fission products due to its low yield as well as analysis on a LEPS or low-energy germanium(LEGa) detector for the low-energy gamma emissions. The results from all Flattop campaigns are shown in Figure 6.19 and Table 6.20. The results highlight the difficulty in the measurement of the fission product. Only three reported values for DU targets exist—from FY 2017, FY 2018, and FY 2021—and in all cases, the determined R-value is less than the ENDF R-value. Conversely, the results from the HEU seems to highlight the improvements to the chemistry and analysis. Where there is variation in the HEU R-values over the campaigns, the R-values coalesce on the ENDF R-value. An R-value nearly identical to the ENDF value with a lower uncertainty was found in FY 2021. This sample was used along with other low-energy samples as long-term calibration sources for the new LEGa detectors, a new acquisition that had not been rigorously tested.

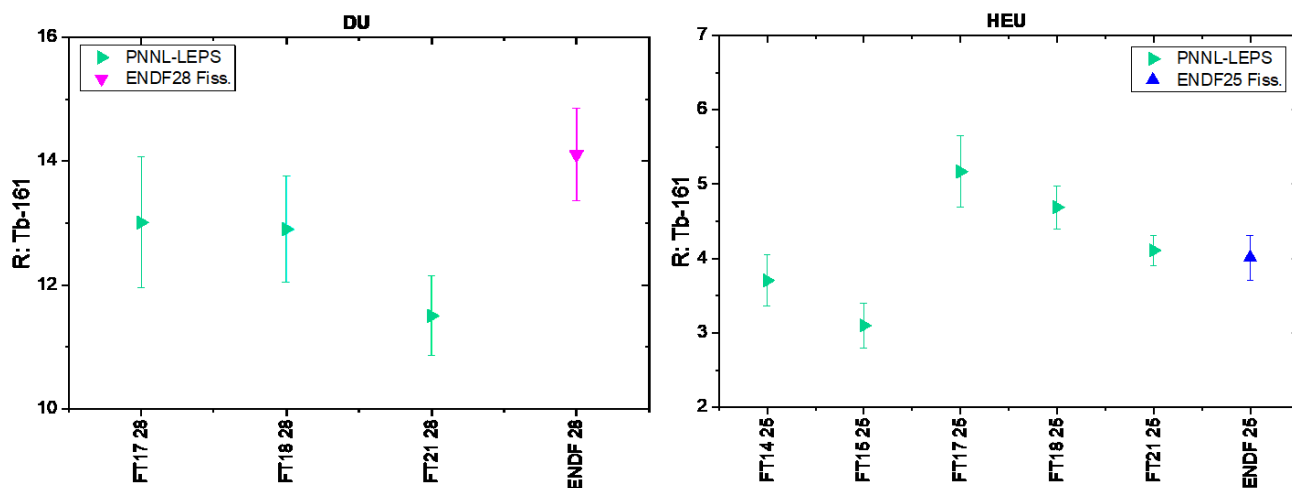


Figure 6.19. Terbium-161 R-values for DU and HEU samples irradiated on the Flattop compared to previous R-value campaigns and ENDF ($R \pm 1\sigma$).

Table 6.20. Terbium-161 R-values for DU and HEU samples irradiated on the Flattop critical assembly compared to previous R-value campaigns and ENDF ($R \pm 1\sigma\%$).

DU							
	FY 2013	FY 2014	FY 2015	FY 2017	FY 2018	FY 2021	ENDF
LEPS	N/A	N/A	N/A	$13.01 \pm 8.11\%$	$12.9 \pm 6.62\%$	$11.5 \pm 5.59\%$	$14.1 \pm 5.27\%$
HEU							
	FY 2013	FY 2014	FY 2015	FY 2017	FY 2018	FY 2021	ENDF
LEPS	N/A	$3.71 \pm 9.26\%$	$3.25 \pm 10.2\%$	$5.17 \pm 9.27\%$	4.69	$4.11 \pm 6.15\%$	$4.01 \pm 4.92\%$

LEPS = low energy photon spectroscopy

6.20 Uranium-237

Uranium-237 radiometric analysis was performed by GEA of A solution and GEA of the separated fractions with yielding of the separated fraction using KPA. Elution of U was accomplished using the methods described in Uhnak et al. (2021b), producing yields higher than previous campaigns. The presence of ^{235}U in the DU target, created an opportunity for the ^{235}U to be used as an internal tracer, allowing for GEA-based yielding of the U. The isotopic composition of the targets can be found in Table 2.2.

Unlike other neutron energies, the cross section for the n,2n reaction that produces ^{237}U from a ^{238}U target is very low. There were detectable quantities of ^{237}U in FY 2021, though comparisons to previous campaign values are difficult as they were not reported in previous fission spectrum irradiation campaigns. A total of 1.28×10^{11} atoms/g of the target were detected, a ratio of $0.0471 \pm 4.1\%$ atoms/fission.

For the FY 2021 irradiation, the HEU target was not isotopically pure with the remainder of the 93% ^{235}U being made up of mostly ^{238}U . Breeding ^{237}U from ^{235}U is unlikely due to the low capture cross section of both the ^{235}U and ^{236}U . The presence of 0.2592% ^{236}U creates a second pathway. A total ^{237}U in the HEU target was $1.28 \times 10^{10} \pm 2.8\%$ atoms/g target were detected,

corresponding to $7.52 \times 10^{-4} \pm 3.8\%$ atoms/fission. It is possible that the production proceeds through both pathways.

6.21 Neptunium-239

Radiometric analysis of ^{239}Np was conducted using GEA of the A solution at PNNL, and from the separated fractions, yielding by GEA of ^{237}Np . Neptunium-239 is produced through the neutron capture on a ^{238}U , with a cross section 1/20th to 1/10th of the fission cross section. Due to the isotopic purity of the targets, there is only a single pathway to produce ^{239}Np , the capture of a neutron on ^{238}U . In the DU target a total of $1.50 \times 10^{12} \pm 4.1\%$ atoms/g target was produced, corresponding to $0.553 \pm 5.7\%$ atoms/fission. In the HEU target, containing about 5% ^{238}U , a total of $7.22 \times 10^9 \pm 3.3\%$ atoms/g target was produced, corresponding to $4.24 \times 10^{-3} \pm 4.1\%$ atoms/fission.

7.0 Result Highlights

As referenced in (Uhnak 2021a) the agreement between PNNL and LANL results were excellent for nearly all isotopes examined.

An excellent agreement between the literature and LANL results (as noted in Uhnak et al. 2021a) was also achieved.

The following adjustments to the chemistry allowed a significant improvement to the full timeline of the campaign:

- An alternative elution condition, using a citrate buffered HEDTA solution was used for the elution of U. This resulted in a smaller elution volume and a greater than twofold increase in the chemical yield.
- A separation method for the rare earth elements, originally developed by collaborators at the Atomic Weapons Establishment in the United Kingdom, was used. This separation method employs extraction chromatography aided by a vacuum box. All rare earth fractions were collected in sufficiently radiopure condition and in high enough yield to meet or exceed those obtained from the traditional chemistry.

Fission yields were calculated for a number of fission products including ^{91}Y and ^{136}Cs .

8.0 Lessons Learned

Yttrium stable analysis is complicated by an unknown source of Y contamination. For future campaigns a ^{88}Y radiotracer has been acquired.

The method used in the FY 2021 campaign will be further developed and the source of the stable Y present will be investigated further.

9.0 Literature R-values

Table 9.1 includes calculated literature R-values with associated propagated uncertainty. All literature values are from the ENDF V.III, JENDL, and JEFF databases. Values obtained from England 1993, Shibata 2011, and Santamarina 2009. R-values were calculated using **Error! Reference source not found..**

Table 9.1. Calculated literature R-values for select fission products. R-value and associated uncertainties were propagated from the fission yields of each fission product.

	^{235}U		^{238}U	
	R-value	$\pm\text{s}\%$	R-value	$\pm\text{s}\%$
^{89}Sr	0.950	2.62%	0.578	2.62%
^{90}Sr	0.972	2.33%	0.556	2.62%
^{91}Sr	1.01	2.99%	0.686	2.99%
^{91}Y	1.01	90.53%	0.686	90.53%
^{93}Y	1.01	90.53%	0.767	90.53%
^{95}Zr	1.02	2.62%	0.783	2.80%
^{97}Zr	1.03	3.14%	0.921	3.14%
^{95}Nb	1.02	2.52%	0.78	2.62%
^{97}Nb	1.03	2.33%	0.92	2.43%
^{99}Mo	1.00	2.80%	1.000	2.80%
^{103}Ru	1.10	2.80%	2.050	2.80%
^{105}Rh	1.28	3.97%	4.16	3.45%
^{111}Ag	2.51	5.27%	4.046	4.89%
^{112}Ag	2.97	6.91%	4.245	7.48%
^{115}Cd	2.76	6.91%	2.946	6.63%
^{115m}Cd	2.86	23.85%	3.065	8.71%
^{124}Sb	36.87	90.53%	1.36	90.53%
^{129m}Te	1.58	32.10%	1.84	11.26%
^{131m}Te	1.07	45.22%	0.63	16.61%
^{132}Te	1.12	3.14%	1.182	2.80%
^{136}Cs	2.18	90.53%	0.172	90.53%
^{137}Cs	1.03	2.10%	0.969	2.27%
^{140}Ba	0.989	2.43%	0.927	2.33%
^{141}Ce	1.05	3.57%	0.904	3.57%
^{143}Ce	0.989	2.80%	0.769	2.80%
^{144}Ce	0.985	2.52%	0.819	2.52%
^{147}Nd	0.979	2.62%	1.143	2.80%
^{149}Pm	0.99	3.14%	1.49	3.45%
^{151}Pm	1.01	2.90%	1.89	3.45%
$^{153}\text{Sm}^*$	1.27	6.47%	3.04	5.47%
^{156}Sm	1.40	8.70%	5.075	9.16%
^{154}Eu	0.33	90.53%	0.042	90.53%
^{155}Eu	1.26	11.87%	4.361	16.61%
^{156}Eu	1.40	4.89%	5.070	4.89%

^{161}Tb	4.01	7.48%	14.107	5.27%
-------------------	------	-------	--------	-------

Table 9.1. (contd.)

91Y	^{235}U		^{238}U	
	R-value	$\pm\text{s}\%$	R-value	$\pm\text{s}\%$
ENDF/B-VII.1	1.01	90.53%	0.69	90.53%
JEFF-3.1.1 (400 keV)	0.94	3.17%	0.70	3.95%
JENDL/FPY-2011	1.01	2.56%	0.68	3.02%
JENDL-4.0	1.01	2.55%	0.68	2.98%
<hr/>				
115mCd	R-value	$\pm\text{s}\%$	R-value	$\pm\text{s}\%$
ENDF/B-VII.1	2.86	23.85%	3.06	8.71%
JEFF-3.1.1 (400 keV)	2.41	18.94%	3.55	14.83%
JENDL/FPY-2011	2.90	23.85%	3.88	8.71%
JENDL-4.0	2.77	62.01%	2.97	85.08%

10.0 Specific Recommendations

The recommendations are as follows:

- A fresh solution of oxidant must be used for the Ce separation.
- Continued use of a complexant for uranium separation is warranted.
- Continued use of the vacuum box lanthanide separation is warranted with minor adjustments to the procedure.
- A radioactive Y tracer is needed for Y yielding; therefore, a ^{88}Y standard has been purchased for this use. It will require a cleaning procedure to remove stable ^{88}Sr prior to use to make sure there is no possible interference with the TIMS analysis.
- The contaminant source of the Y will be further investigated. The stable Y determination via ICP-MS is the backup yielding method if ^{88}Y is not available.

11.0 Conclusions

Collaborating with LANL, PNNL performed six fission energy neutron irradiation campaigns, in FY 2013, FY 2014, FY 2015, FY 2017, FY 2018, and FY 2021. In each campaign, one of the Flattop critical assemblies were used for the irradiation. Both HEU and DU were irradiated in each campaign.

Comparing the individual campaigns has shown PNNL analysis results to be highly consistent with the established literature values. Analysis at multiple laboratories with multiple analytical techniques and near replicate irradiations improves the confidence in the data produced in these campaigns and highlights areas that require improvements.

This work used improved chemistries and analytical techniques compared to methodologies used for the literature data, which consequently provided improvements to the overall CFY and/or the associated uncertainty. The campaigns at the various neutron facilities provide the opportunity to maintain the current radiochemistry capability and grow the unique capabilities at the national laboratories.

12.0 References

Canberra Industries, Inc. 2006. *Genie™ 2000 Spectroscopy Software, Operations*. Canberra Industries, Inc., Meriden, Connecticut.

<https://www3.nd.edu/~wzech/Genie%202000%20Operations%20Manual.pdf>

Chadwick M.B., M. Herman, P. Obložinský, M.E. Dunn, Y. Danon, A.C. Kahler, D.L. Smith, B. Pritychenko, G. Arbanas, R. Arcilla, R. Brewer, D.A. Brown, R. Capote, A.D. Carlson, Y.S. Cho, H. Derrien, K. Guber, G.M. Hale, S. Hoblit, S. Holloway, T.D. Johnson, T. Kawano, B.C. Kiedrowski, H. Kim, S. Kunieda, N.M. Larson, L. Leal, J.P. Lestone, R.C. Little, E.A. McCutchan, R.E. MacFarlane, M. MacInnes, C.M. Mattoon, R.D. McKnight, S.F. Mughabghab, G.P.A. Nobre, G. Palmiotti, A. Palumbo, M.T. Pigni, V.G. Pronyaev, R.O. Sayer, A.A. Sonzogni, N.C. Summers, P. Talou, I.J. Thompson, A. Trkov, R.L. Vogt, S.C. van der Marck, A. Wallner, M.C. White, D. Wiarda, P.G. Young. 2011. "ENDF/B-VII.1 Nuclear Data for Science and Technology: Cross Sections, Covariances, Fission Product Yields and Decay Data." *Nuclear Data Sheets*, 112(12):2887-2996. <https://doi.org/10.1016/j.nds.2011.11.002>.

Degnan D.J., A. Bilbao Pena, L.M. Bramer, and L. McCue. 2019. *Tools to Visualize Post-Translational Modifications from Tandem LC-MS Data*. PNNL-29454. Pacific Northwest National Laboratory, Richland, Washington.

England, T.R. and B. F. Rider. 1994. *Evaluation and Compilation of Fission Product Yields* 1993. LA-UR-94-3106, Los Alamos National Laboratory, Los Alamos, New Mexico.
<https://t2.lanl.gov/nis/publications/endf349.pdf>

Jackson M.J.; C. Gilligan, A.V. Davies, R. Britton, J.I. Friese, L.R. Greenwood, R.D. Pierson, Z.S. Finch, B.N. Gartman, D. Dry, I. May, N.C. Smythe, A.J. Gaunt, E.R. Thomas, K.E. Roberts, N.K. Harward, K.J. Thomas, P.T. Woody, and P. Zhao. 2018. "International Inter-comparison Exercise on ¹⁵³Sm." *Journal of Radioanalytical and Nuclear Chemistry*, 318(1):107-115. doi:10.1007/s10967-018-6048-1

Santamarina A., D. Bernard, P. Blaise, M. Coste, A. Courcelle, D. Huynh, C. Jouanne, P. Leconte, O. Litaize, S. Mengelle, G. Noguere, J-M. Ruggiere, O Serot, J. Tommasi, C. Vaglio, and J-F. Vidal. 2009. *The JEFF 3.1.1 Nuclear Data Library*. *JEFF Report 22, Validation Results from JEF-2.2 to JEFF 3.1.1*. Nuclear Energy Agency. Organisation for Economic Co-operation and Development. https://www.oecd-nea.org/jcms/pl_14470/the-jeff-3-1-1-nuclear-data-library?details=true

Seiner D.R., B.N. Gartman, M.M. Haney, B.D. Pierson, B. Archambault, J.H. Estrada, J.I. Friese, J.I. 2020. *PNNL After Action Report for the Thermal Calibration (QA-PFTP-2021-02)* PNNL-X-900-2189. Pacific Northwest National Laboratory, Richland, Washington.

Shibata K., O. Iwamoto, T. Nakagawa, N. Iwamoto, A. Ichihara, S Kunieda, S Chiba, K Furutaka, N Otuka, T. Oshawaw, T. Murata, H Matsunobu, A Zukeran, S Kamada, and J. Katafura. 2011. "JENDL-4.0: A New Library for Nuclear Science and Engineering." *Journal of Nuclear Science and Technology*, 48(1):1-30.
<https://doi.org/10.1080/18811248.2011.9711675>

Uhnak N.E., M.M. Haney, B.D. Pierson, L.R. Greenwood, J.I. Friese, L.A. Metz, M. Dembowski, A.J. Gaunt, W.S. Kinman, I. May, D. Meininger, S.D. Reilly, N.C. Smythe, M. Boswell, M.R. James, D.C. Flanagan, C Magiotta, J.L. Miller, J.M. White, M.S. Wren, L.S. Hudson, R.J. Rendon, G. Lee, D.L. Cox III, C. C. Lance, J.R. Romero, and J.M. Williams. 2021a. *April 2021 NCERC Irradiation – Target Preparation and Post-irradiation Radiochemical Analysis*. PNNL-32008. Pacific Northwest National Laboratory, Richland, Washington. [Limited Distribution]

Uhnak N.E., M.M. Haney, L.M. Arrigo, L.R. Greenwood, B.D. Pierson, J.I. Friese, and L.A. Metz. 2021b. *FY20 R-value Measurement Results for 14 MeV Neutron Irradiation of DU and HEU Targets*. PNNL-31327. Pacific Northwest National Laboratory, Richland, Washington.

Uhnak N.E., M.M. Haney, B.D. Pierson, L.R. Greenwood, J.I. Friese, and L.A. Metz. 2021. *R-Value Measurements Performed in FY21 on Uranium Targets Irradiated by Fission Spectrum Neutrons*. PNNL-31718. Pacific Northwest National Laboratory, Richland, Washington.

Appendix A – PNNL Calculations and Associated Uncertainty

A.1 A Solution GEA

A.1.1 Atoms per Gram A Solution

Each A solution was analyzed by gamma energy analysis (GEA) multiple times; corrections were applied for decay during irradiation using the irradiation history of each measurement. The reported atoms per gram A solution (N/g A) for each isotope is the weighted average of the applicable counts using the formula shown in Eq. A.1; any counts that had interferences or very high uncertainty due to decay were discarded.

The uncertainty associated with the activity for each isotope in a GEA is provided by the Genie 2000 software (Canberra Industries 2006) and considers the counting statistics, the counting efficiency, and other applicable factors as described in the operator's manual. The weighted uncertainty for the average N/g A was calculated using Equations Eq. A.2 and Eq A.3. The unweighted uncertainty for the average N/g A is calculated using the stdev.S function in Excel which uses the “n-1” method. The weighted and unweighted % relative standard deviation (RSD) values were compared, and the higher value, which was typically the unweighted value, was reported. Example data are shown in Table A.1.

$$\text{Average}_{\text{wtd}} = \frac{\frac{N_1}{\sigma_1^2} + \frac{N_2}{\sigma_2^2} + \frac{N_3}{\sigma_3^2}}{\frac{1}{\sigma_1^2} + \frac{1}{\sigma_2^2} + \frac{1}{\sigma_3^2}} \quad (\text{Eq. A.1})$$

$$\sigma_{\text{wtd}} = \frac{1}{\frac{1}{\sigma_1^2} + \frac{1}{\sigma_2^2} + \frac{1}{\sigma_3^2}} \quad (\text{Eq. A.2})$$

$$\% \text{RSD}_{\text{wtd}} = \frac{\sigma_{\text{wtd}}}{\text{Average}_{\text{wtd}}} \quad (\text{Eq. A.3})$$

Where

N is the atoms per gram of A solution

σ is the uncertainty

%RSD is the relative standard deviation

wtd is weighted

Table A.1. Atoms per gram of A solution for Zr-97 in four A solution counts

	N/g A	$\pm 1\sigma$	%RSD _W (Weighted)	% RSD _U (Unweighted)
Count 1	2.67×10^9	3.45×10^7		
Count 2	2.66×10^9	4.25×10^7		
Count 3	2.77×10^9	7.59×10^7		
Count 4	2.82×10^9	7.09×10^7		
Weighted Average	2.69×10^9	2.38×10^7	$\pm 0.883\%$	$\pm 2.89\%$

A.2 R-value

The R-value was calculated using Eq. 1 or Eq. 2 (Section 4.0), which is repeated below in Eq. A.4 along with the applicable uncertainty shown in Eq. A.5.

$$R = \frac{\frac{N_X}{N_{Mo99}}}{r_{hist}} \text{ or } \frac{\frac{N_X}{N_{Mo99}}}{\left(\frac{CFY_X}{CFY_{Mo99}}\right)_{U235 \text{ thermal}}} \quad (\text{Eq. A.4})$$

$$\sigma_R = \sqrt{\sigma_{N_X}^2 + \sigma_{N_{Mo99}}^2} \text{ or } \sqrt{\sigma_{N_X}^2 + \sigma_{N_{Mo99}}^2 + \sigma_{CFY_X}^2 + \sigma_{CFY_{Mo99}}^2} \quad (\text{Eq. A.5})$$

A.3 Absolute Fission Yield Calculation Example

Equation 3 (Section 6.2) is repeated in Eq. A.6, with the intention of demonstrating its use in the calculation of the absolute fission yield for ^{136}Cs .

$$CFY_X = \frac{Atoms_X/g}{Fissions/g} \quad (\text{Eq. A.6})$$

$$CFY_{Cs136\text{thermal}} = \frac{Atoms_{Cs136}/g}{Fissions/g} = \frac{2.04 \times 10^8 \pm 3.7\% \text{ atoms/g}}{3.53 \times 10^{12} \pm 3.1\% \text{ fission/g}} = 5.78 \times 10^{-5} \pm 7.6\%$$

$$CFY_{Cs136\text{fission}} = \frac{Atoms_{Cs136}/g}{Fissions/g} = \frac{7.65 \times 10^6 \pm 2.0\% \text{ atoms/g}}{5.97 \times 10^{10} \pm 2.5\% \text{ fission/g}} = 1.28 \times 10^{-4} \pm 3.2\%$$

A.3.1 Relative Fission Yield Calculation Example

The R-value equation can be replaced with one containing only the cumulative fission yields (CFYs) for ^{99}Mo at different energies and the analyte of interest X as shown in Eq. A.7. The relative fission yield can then be calculated using by rearranging Eq. A.7.

$$R = \frac{\left(\frac{CFY_X}{CFY_{Mo99}}\right)_{fission}}{\left(\frac{CFY_X}{CFY_{Mo99}}\right)_{U235 \text{ thermal}}} \quad (\text{Eq. A.7})$$

Rearrangement of Eq. A.7, the R-value used in the calculation of the relative fission yield is the average of all measured R-values for all fission spectrum campaigns that have been completed (see Table 6.11 for values used). The CFY used for thermal fission of ^{235}U for ^{136}Cs was calculated using the values measured from the FY 2021 thermal calibration campaign.

$$CFY_{X\text{fission}} = R \times \frac{CFY_{Mo99\text{fission}} \times CFY_{X\text{th}}}{CFY_{Mo99\text{th}}} \quad (\text{Eq. A.8})$$

$$CFY_{136\text{Cs}\text{fission}} = 2.29 \pm 4.1\% \times \frac{5.94 \times 10^{-2} \pm 1.4\% \times 5.78 \times 10^{-5} \pm 6.76\%}{6.11 \times 10^{-2} \pm 1.4\%} = 1.36 \times 10^{-4} \pm 8.1\%$$

A.4 Separated Fractions

The separated fractions are analyzed by one or more analytical techniques including GEA, inductively coupled plasma optical emission spectroscopy (ICP-OES), inductively coupled plasma mass spectrometry (ICP-MS), kinetic phosphorescence analysis (KPA), and/or liquid scintillation counting (LSC). Each technique has different uncertainty considerations.

- The uncertainty associated with the activity for each isotope in a GEA is provided by the Genie 2000 software (Canberra Industries 2006) and takes into account the counting statistics, the counting efficiency, and other applicable factors as described in the manual.
- The uncertainty for ICP-OES was calculated using two sources of uncertainty. The first source is the overall repeatability of the method and instrument response, this appears to be the largest contributor to the overall uncertainty. The repeatability represents the standard deviation of the percent recovery for a series of check solutions that were analyzed every other week for the last year. The other source was the uncertainty of the certified calibration standard, which contributes to the uncertainty of the calibration process. The two uncertainties were added in quadrature, $U = \sqrt{u_1^2 + u_2^2}$. One source of uncertainty, which was evaluated but not included, was dilutions of the standard during preparation, since this was done gravimetrically with a high-precision, calibrated balance, the uncertainty was considered negligible.
- The uncertainty for ICP-MS is based on the instrument reported RSD of three replicate sample measurements.
- The uncertainty for KPA is determined by the KPAwin version 1.2.9 software.
- The uncertainty for each isotope in an LSC analysis is based on the square root of the number of counts, where applicable the counting efficiency for ^{89}Sr and ^{161}Tb is assumed to be 100%.

A.4.1 Tracer Analysis

An aliquot of each radioactive and stable tracer used for chemical yielding for the separated fractions was analyzed to determine the amount of analyte present per mass of the tracer solution. The analytical result was used to calculate the amount of tracer added to each replicate rather than a certificate value. The solutions were prepared using a four-place calibrated analytical balance; the uncertainty associated with the mass measurement is not included in the uncertainty propagation.

A.4.2 Yield

Each replicate was spiked with radioactive and/or stable tracers to enable chemical yield corrections. The yield was calculated by comparing the tracer value in the sample to the tracer value from the stock analysis; the average yield is reported but not used in the calculations since calculations for each replicate use the applicable replicate yield. The uncertainty for the yield was calculated using the standard uncertainty equations for multiplication and division as shown in Eq. 9). The relative uncertainty (in percent) on the yield is then given by:

$$\sigma_{\text{rel}}(\%) = \sqrt{\sigma_1^2 + \sigma_2^2 + \dots} = \sqrt{\sigma_{\text{sample}}^2 + \sigma_{\text{tracer}}^2} \quad (\text{Eq. A.9})$$

If a replicate is spiked with 0.2225 g ^{109}Cd tracer with a concentration of $1.66 \times 10^4 \pm 3.00\%$ Bq/g tracer solution and the measured value is $3.61 \times 10^3 \pm 2.96\%$ Bq/sample then the yield is $97.7 \pm 4.22\%$

$$\text{Yield} = \frac{3.61 \times 10^3 \text{ Bq/sample}}{0.2225 \text{ g tracer}} * \frac{1}{1.66 \times 10^4 \text{ Bq/g tracer solution}} = 78.0\%$$

$$\sigma_{\text{yield}} = \sqrt{(3.00\%)_{\text{sample}}^2 + (2.96\%)_{\text{tracer}}^2} = 4.22\%$$

A.4.3 Atoms per Gram of A Solution

The analyte of interest in each replicate was converted from Bq/sample to a yield corrected N/g A solution as given in Eq. A.10 with the uncertainty given in Eq. A.11. Lambda is the decay constant for the given isotope.

$$\text{N of X per g A} = \frac{\text{Bq of X per separated fraction}}{\text{mass of A solution}} * \frac{1}{\text{Yield}} * \frac{1}{\text{lambda of X}} \quad (\text{Eq. A.10})$$

$$\text{relative uncertainty (\%)} = \sigma_{\text{rel}} = \sqrt{\sigma_1^2 + \sigma_2^2 + \dots} = \sqrt{\sigma_{\text{Bq of X}}^2 + \sigma_{\text{yield}}^2} \quad (\text{Eq. A.11})$$

If a replicate containing 4.7134 g A solution was found to have $1.05 \times 10^3 \pm 1.50\%$ Bq/sample ^{115}Cd and a yield of $97.7 \pm 4.22\%$ then the ^{115}Cd N/g A solution is $6.33 \times 10^7 \pm 4.47\%$.

$$\text{N/g A } ^{115}\text{Cd} = \frac{1.05 \times 10^3 \text{ Bq/sample}}{4.7134 \text{ g A solution}} * \frac{1}{97.7\%} * \frac{1}{3.60 \times 10^{-6} \text{ s}^{-1}} = 6.33 \times 10^7 \text{ N/g A solution}$$

$$\sigma_{\text{N/g A}} = \sqrt{(1.50\%)_{\text{Bq of X}}^2 + (4.22\%)_{\text{yield}}^2} = 4.47\%$$

For samples with more than one replicate the average N/g A solution was used for calculating the R-value for a given isotope. The uncertainty for the average is given in Eq. A.12 where S is the sample quantity (i.e., N/g A) and σ is the relative uncertainty for each S in %.

$$\sigma_{\text{ave}} (\%) = \frac{\sqrt{(S_1 * \sigma_1)^2 + (S_2 * \sigma_2)^2 + \dots}}{\sqrt{\# \text{ of reps}}} * 100 \quad (\text{Eq. A.12})$$

If two replicates are found to have $6.33 \times 10^7 \pm 4.47\%$ and $5.73 \times 10^7 \pm 4.37\%$ N/g A solution ^{115}Cd , respectively, then the average is $6.03 \times 10^7 \pm 4.43\%$ N/g A solution.

$$\sigma_{\text{ave}} = \frac{\sqrt{(6.33 \times 10^7 * 4.47\%)^2 + (5.73 \times 10^7 * 4.37\%)^2}}{\sqrt{2}} * 100 = 4.43\%$$

A.4.4 R-value

The R-value and uncertainty are calculated in the same manner as given in Eq. A.4 and Eq. A.5. The uncertainty for r_{hist} was not included. The uncertainty for values from ENDF/B-VII.I (Chadwick et al. 2011, have been included if the uncertainty for the CFY is less than 64%; 64% propagates to an uncertainty of around 90% for the R-value, which is rather meaningless and only affects ^{91}Y , ^{93}Y , and ^{136}Cs .

If two replicates are found to have an average of $6.03 \times 10^7 \pm 4.43\%$ N/g A for ^{115}Cd and $4.08 \times 10^8 \pm 2.15\%$ N/g A for ^{99}Mo and the r_{hist} for ^{115}Cd is 2.07×10^{-3} then the R-value is $71.5 \pm 4.93\%$.

$$R = \frac{\frac{6.03 \times 10^7 \text{ N/g A solution } ^{115}\text{Cd}}{4.08 \times 10^8 \text{ N/g A solution } ^{99}\text{Mo}}}{2.07 \times 10^{-3}} = 71.5$$

$$\sigma_R = \sqrt{(4.43\%)^2 + (2.15\%)^2} = 4.93\%$$

A.4.5 Atoms per Fission

Activation products such as ^{237}U and ^{239}Np are reported in atoms per fission. The N/f and associated uncertainty is calculated in the same manner as given in Eq. A.4 and Eq. A.5.

$$\text{N of X per fission} = \text{N of X per g A} * \frac{1}{\text{fissions per g A}} \quad (\text{Eq. A.13})$$

$$\text{relative uncertainty (\%)} = \sigma_{\text{rel}} = \sqrt{\sigma_1^2 + \sigma_2^2 + \dots} = \sqrt{\sigma_{\text{N/g A}}^2 + \sigma_{\text{f/g A}}^2} \quad (\text{Eq. A.14})$$

If a replicate was found to have $1.46 \times 10^8 \pm 3.16\% \text{ N/g A}^{239}\text{Np}$ and $6.68 \times 10^9 \pm 2.57\% \text{ f/g A}$, then the ^{239}Np N/f is $2.19 \times 10^{-2} \pm 4.07\%$.

$$\text{N/f } ^{239}\text{Np} = 1.46 \times 10^8 \text{ N/g A} * \frac{1}{6.68 \times 10^9 \text{ f/g A}} = 2.19 \times 10^{-2} \text{ N/f}$$

$$\sigma_{\text{N/f}} = \sqrt{(3.16\%)_{\text{N/g A}}^2 + (2.57\%)_{\text{f/g A}}^2} = 4.07\%$$

Pacific Northwest National Laboratory

902 Battelle Boulevard
P.O. Box 999
Richland, WA 99354

1-888-375-PNNL (7665)

www.pnnl.gov